



# Partitioning of canopy and soil CO<sub>2</sub> fluxes in a pine forest at the dry timberline across a 13-year observation period

Rafat Qubaja, Fyodor Tatarinov, Eyal Rotenberg, and Dan Yakir

Department of Earth and Planetary Sciences, Weizmann Institute of Science, Rehovot 76100, Israel

**Correspondence:** Dan Yakir (dan.yakir@weizmann.ac.il)

Received: 25 July 2019 – Discussion started: 31 July 2019

Revised: 12 December 2019 – Accepted: 6 January 2020 – Published: 11 February 2020

**Abstract.** Partitioning carbon fluxes is key to understanding the process underlying ecosystem response to change. This study used soil and canopy fluxes with stable isotopes (<sup>13</sup>C) and radiocarbon (<sup>14</sup>C) measurements in an 18 km<sup>2</sup>, 50-year-old, dry (287 mm mean annual precipitation; nonirrigated) *Pinus halepensis* forest plantation in Israel to partition the net ecosystem's CO<sub>2</sub> flux into gross primary productivity (GPP) and ecosystem respiration ( $R_e$ ) and (with the aid of isotopic measurements) soil respiration flux ( $R_s$ ) into autotrophic ( $R_{sa}$ ), heterotrophic ( $R_h$ ), and inorganic ( $R_i$ ) components. On an annual scale, GPP and  $R_e$  were 655 and 488 g C m<sup>-2</sup>, respectively, with a net primary productivity (NPP) of 282 g C m<sup>-2</sup> and carbon-use efficiency (CUE = NPP / GPP) of 0.43.  $R_s$  made up 60 % of the  $R_e$  and comprised 24 ± 4 %  $R_{sa}$ , 23 ± 4 %  $R_h$ , and 13 ± 1 %  $R_i$ . The contribution of root and microbial respiration to  $R_e$  increased during high productivity periods, and inorganic sources were more significant components when the soil water content was low. Comparing the ratio of the respiration components to  $R_e$  of our mean 2016 values to those of 2003 (mean for 2001–2006) at the same site indicated a decrease in the autotrophic components (roots, foliage, and wood) by about −13 % and an increase in the heterotrophic component ( $R_h/R_e$ ) by about +18 %, with similar trends for soil respiration ( $R_{sa}/R_s$  decreasing by −19 % and  $R_h/R_s$  increasing by +8 %, respectively). The soil respiration sensitivity to temperature ( $Q_{10}$ ) decreased across the same observation period by 36 % and 9 % in the wet and dry periods, respectively. Low rates of soil carbon loss combined with relatively high belowground carbon allocation (i.e., 38 % of canopy CO<sub>2</sub> uptake) and low sensitivity to temperature help explain the high soil organic carbon accumulation and the relatively high ecosystem CUE of the dry forest.

## 1 Introduction

The annual net storage of carbon in the land biosphere, known as net ecosystem production (NEP), is the balance between carbon uptake during gross primary productivity (GPP) and carbon loss during growth, maintenance respiration by plants (i.e., autotrophic respiration,  $R_a$ ), and decomposition of litter and soil organic matter (i.e., heterotrophic respiration,  $R_h$ ; Bonan, 2008). The difference between GPP and  $R_a$  expresses the net primary production (NPP) and is the net carbon uptake by plants that can be used for new biomass production. Measurements from a range of ecosystems have shown that total plant respiration can be as large as 50 % of GPP (e.g., Etzold et al., 2011) and together with  $R_h$  comprises total ecosystem respiration ( $R_e$ ;  $R_e = R_a + R_h$ ). The partitioning of the ecosystem carbon fluxes can therefore be summarized as

$$\text{GPP} = \text{NPP} + R_a = \text{NEP} + R_h + R_a. \quad (1)$$

Earlier campaign-based measurements carried out by Maseyk et al. (2008a) and Grünzweig et al. (2009) in the semiarid *Pinus halepensis* (Aleppo pine) Yatir Forest indicated that GPP at this site was lower than among temperate coniferous forests (1000–1900 g C m<sup>-2</sup> yr<sup>-1</sup>) but within the range estimated for Mediterranean evergreen needleleaf and boreal coniferous forests (Falge et al., 2002; Flechard et al., 2019b) and had a high carbon-use efficiency (CUE) of 0.4 (CUE = NPP / GPP; DeLucia et al., 2007). The total flux of CO<sub>2</sub> released from the ecosystem ( $R_e$ ) can be partitioned into aboveground autotrophic respiration (i.e., foliage and sapwood,  $R_f$ ) and soil CO<sub>2</sub> flux ( $R_s$ ).  $R_s$ , in turn, is a combination of three principal components and can be further partitioned into the components originating from

roots or rhizospheres and mycorrhizas (i.e.,  $R_{sa}$ ), from carbon respired during the decomposition of dead organic matter by soil microorganisms and macrofauna ( $R_h$ ; Bahn et al., 2010; Kuzyakov, 2006), and from pedogenic or anthropogenic acidification of soils containing CaCO<sub>3</sub> ( $R_i$ ; Joseph et al., 2019; Kuzyakov, 2006), which is expressed as

$$R_e = R_s + R_f = [R_{sa} + R_h + R_i] + R_f. \quad (2)$$

Previously published results show that the contribution of  $R_{sa}$  and  $R_h$  to  $R_s$  ranges from 24 % to 65 % and from 29 % to 74 %, respectively, in forest soils in different biomes and ecosystems (Binkley et al., 2006; Chen et al., 2010; Flechard et al., 2019a; Frey et al., 2006; Hogberg et al., 2009; Subke et al., 2011). Some studies reported significant proportions of abiotic contribution to  $R_s$ , ranging between 10 % and 60 % (Martí-Roura et al., 2019; Ramnarine et al., 2012; Joseph et al., 2019). However, most of these experiments were performed in boreal, temperate, or subtropical forests, and there is a general lack of information on water-limited environments, such as dry Mediterranean ecosystems. Using both <sup>13</sup>C and CO<sub>2</sub>/O<sub>2</sub> ratios also showed that abiotic processes, such as CO<sub>2</sub> storage, transport, and interactions with sediments, can influence  $R_s$  measurements at such sites (Angert et al., 2015; Carmi et al., 2013). Furthermore, root-respired CO<sub>2</sub> can also be dissolved in the xylem water and carried upward with the transpiration stream (Etzold et al., 2013).

Rates of the soil–atmosphere CO<sub>2</sub> flux ( $R_s$ ) have been altered owing to global climatic change, particularly through changes in soil temperature ( $T_s$ ) and soil moisture (SWC; Bond-Lamberty and Thomson, 2010; Buchmann, 2000; Carvalhais et al., 2014; Hagedorn et al., 2016; Zhou et al., 2009), which could account for 65 %–92 % of the variability of  $R_s$  in a mixed deciduous forest (Peterjohn et al., 1994). Soil moisture impacts on  $R_s$  have been observed in arid and Mediterranean ecosystems, where  $T_s$  and SWC are negatively correlated (e.g., Grünzweig et al., 2009). CO<sub>2</sub> efflux generally increases with increasing soil temperatures (Frank et al., 2002), which can produce positive feedback on climate warming (Conant et al., 1998), converting the biosphere from a net carbon sink to a carbon source (IPCC, 2014). A range of empirical models have been developed to relate  $R_s$  rate and temperature (Balogh et al., 2011; Lellei-Kovács et al., 2011), and the most widely used models rely on the  $Q_{10}$  approach (Bond-Lamberty and Thomson, 2010), which quantifies the sensitivity of  $R_s$  to temperature and can integrate it with physical processes, such as the rate of O<sub>2</sub> diffusion into and CO<sub>2</sub> diffusion out of soils and the intrinsic temperature dependency of enzymatic processes (Davidson and Janssens, 2006). Soil moisture (SWC) may be of greater importance than temperature in influencing  $R_s$  in water-limited ecosystems (Hagedorn et al., 2016; Grünzweig et al., 2009; Shen et al., 2008). In general, the  $R_s$  rate increases with the increase of SWC at low levels but decreases at high levels of SWC (Deng et al., 2012; Hui and Luo, 2004; Jiang et al., 2013). Several studies

highlight the sensitivity of carbon fluxes in semiarid Mediterranean ecosystems to the irregular seasonal and interannual distribution of rain events (Poulter et al., 2014; Ross et al., 2012). While  $R_s$  is generally constrained by low SWC during summer months, abrupt and large soil CO<sub>2</sub> pulses have been observed after rewetting the dry soil (Matteucci et al., 2015).

The objectives were twofold: first, to obtain detail on partitioning of the carbon fluxes in a semiarid pine forest to help explain the high productivity and carbon use efficiency recently reported for this ecosystem (Qubaja et al., 2019) and provide process-based information to assess the carbon sequestration potential of such a semiarid afforestation system; and second, to combine this 2016 study with the results of a similar one at the same site in 2003 (mean values for 2001–2006; Grünzweig et al., 2007, 2009) to obtain a long-term perspective across 13 years on soil respiration and its partitioning. We hypothesized that the high carbon-use efficiency of the dry-forest ecosystem is associated with high below-ground carbon allocation and relatively low decomposition rates and that the long-term trend associated with warming may be suppressed by the dry conditions.

## 2 Materials and methods

### 2.1 Site description

The Yatir Forest (31°20′49″ N, 35°03′07″ E; 650 m a.s.l.) is situated in the transition zone between subhumid and arid Mediterranean climates (Fig. S1 in the Supplement) on the edge of the Hebron mountain ridge. The ecosystem is a semiarid pine afforested area established in the 1960s and covering approximately 18 km<sup>2</sup>. The average air temperatures for January and July are 10.0 and 25.8 °C, respectively. Mean annual potential evapotranspiration (ET) is 1600 mm, and mean annual precipitation is 287 mm. Only winter (December to March) precipitation occurs in this region, creating a distinctive wet season, while summer (June to October) is an extended dry season. There are short transition periods between seasons, with a wetting season (i.e., fall) and a drying season (i.e., spring). The forest is dominated by Aleppo pine (*Pinus halepensis* Mill.), with smaller proportions of other pine species and cypress and little understory vegetation. Tree density in 2007 was 300 trees ha<sup>-1</sup>; mean tree height was 10.0 m; diameter at breast height (DBH) was ~ 15.9 cm, and the leaf area index (LAI) was ~ 1.5. The native background vegetation was sparse shrubland, which is dominated by the dwarf shrub *Sarcopoterium spinosum* (L.) Spach, with patches of herbaceous annuals and perennials reaching a total vegetation height of 0.30–0.50 m (Grünzweig et al., 2003, 2007). The root density range is 30–80 roots m<sup>-2</sup> at the upper 0.1 m soil depth, falling to the minimum value (~ 0 roots m<sup>-2</sup>) at 0.7 m soil depth (Preisler et al., 2019). Biological soil crust (BSC) is evident in the forest but is

less than in the surrounding shrub by  $\sim 40\%$  (Gelfand et al., 2012).

The soil at the research site is shallow (20–40 cm), reaching only 0.7–1.0 m; the stoniness fraction for the soil depth (0–1.2 m) is 15%–60%, and the rock cover of the surface ranges between 9% and 37%, as recently described in detail (Preisler et al., 2019); the soil is eolian-origin loess with a clay–loam texture (31% sand, 41% silt, and 28% clay; density is  $1.65 \pm 0.14 \text{ g cm}^{-3}$ ) overlying chalk and limestone bedrock. Deeper soils (up to 1.5 m) are sporadically located at topographic hollows. While the natural rocky hill slopes in the region are known to create flash floods, the forested plantation reduces runoff dramatically to less than 5% of annual rainfall (Shachnovich et al., 2008). Groundwater is deep ( $> 300 \text{ m}$ ), reducing the possibility of groundwater recharge due to negative hydraulic conductivity or of water uptake by trees from the groundwater.

## 2.2 Flux and meteorological measurements

An instrumented eddy covariance (EC) tower was erected in the geographical center of Yatir Forest, following the EUROFLUX methodology (Aubinet et al., 2000). The system uses a three-dimensional (3-D) sonic anemometer (Omnidirectional R3, Gill Instruments, Lymington, UK) and a closed path LI-7000 CO<sub>2</sub>/H<sub>2</sub>O gas analyzer (LI-COR Inc., Lincoln, NE, USA) to measure the evapotranspiration flux (ET) and net CO<sub>2</sub> flux (NEE). EC flux measurements were used to estimate the annual scale of NEP by integrating half-hourly NEE values. The long-term operation of our EC measurement site (since 2000; see Rotenberg and Yakir, 2010) provides continuous flux and meteorological data with about 80% coverage, which are subjected to  $U^*$  nighttime correction and quality control, and gap filling is based on the extent of the missing data, as recently described in more detail in Tatarinov et al. (2016). A site-specific algorithm was used for flux partitioning into  $R_e$  and GPP. Daytime ecosystem respiration ( $R_e - d$ ; in  $\mu\text{mol m}^{-2} \text{ s}^{-1}$ ) was estimated based on measured nighttime values ( $R_e - n$ ; i.e., when the global radiation was  $< 5 \text{ W m}^{-2}$ ), averaged for the first 3 half hours of each night. The daytime respiration for each half hour was calculated according to Eq. (3) (Maseyk et al., 2008a; Tatarinov et al., 2016):

$$R_{e-d} = R_{e-n} \left( \alpha_1 \beta_s^{dT_s} + \alpha_2 \beta_w^{dT_a} + \alpha_3 \beta_f^{dT_a} \right), \quad (3)$$

where  $\beta_s$ ,  $\beta_w$ , and  $\beta_f$  are coefficients that correspond to soil, wood, and foliage, respectively;  $dT_s$  and  $dT_a$  are soil and air temperature deviations from the values at the beginning of the night; and  $\alpha_1$ ,  $\alpha_2$ , and  $\alpha_3$  are partitioning coefficients fixed at 0.5, 0.1, and 0.4, respectively. The  $\beta_s$ ,  $\beta_w$ , and  $\beta_f$  coefficients were calculated as follows:  $\beta_s$  values were based on  $Q_{10}$  from the Grünzweig et al. (2009) study at the same site, where  $\beta_s = 2.45$  for wet soil (i.e., SWC in the upper 30 cm above 20% vol.);  $\beta_s = 1.18$  for dry soil (i.e., SWC in the upper 30 cm equal to or below 20% vol.);  $\beta_f = 3.15 - 0.036 T_a$ ;

and  $\beta_w = 1.34 + 0.46 \exp(-0.5((\text{DoY} - 162)/66.1)^2)$ , where DoY is the day of the hydrological year starting from 1 October. Finally, GPP was calculated as  $\text{GPP} = \text{NEE} - R_e$ . Negative values of NEE and GPP indicated that the ecosystem was a CO<sub>2</sub> sink.

Half-hourly auxiliary measurements used in this study included photosynthetic activity radiation (PAR;  $\text{mol m}^{-2} \text{ s}^{-1}$ ), vapor pressure deficit (VPD; kPa), wind speed ( $\text{m s}^{-1}$ ), and relative humidity (RH; %), with additional measurements as described elsewhere (Tatarinov et al., 2016). Furthermore, the soil microclimatology half-hourly measurements were measured and calculated with soil chamber measurements, using the LI-8150-203 (LI-COR, Lincoln, NE), as described below, namely air temperature ( $T_a$ ; °C) and relative humidity at 20 cm above the soil surface and soil temperature ( $T_s$ ; °C) at a 5 cm soil depth using a soil temperature probe, as well as volumetric soil water content ( $\text{SWC}_{0-10}$ ;  $\text{m}^3 \text{ m}^{-3}$ ) in the upper 10 cm of the soil near the chambers, using the ThetaProbe model ML2x (Delta-T Devices Ltd., Cambridge, UK), which was calibrated to the soil composition based on the manufacturer's equations.

## 2.3 Soil CO<sub>2</sub> fluxes

Soil CO<sub>2</sub> fluxes ( $R_s$ ) were measured with automated non-steady-state systems, using 20 cm diameter opaque chambers and a multiplexer to allow for simultaneous control of several chambers (LI-8150, -8100-101, -8100-104; LI-COR, Lincoln, NE). The precision of CO<sub>2</sub> measurements in the chambers' air is  $\pm 1.5\%$  of the measurements' range (0–20 000 ppm). The chambers were closed on preinstalled PVC collars of 20 cm diameter, allowing for a short measurement time (i.e., 2 min), and positioned away from the collars for the rest of the time. Data were collected using a system in which air from the chambers was circulated ( $2.5 \text{ L min}^{-1}$ ) through an infrared gas analyzer (IRGA) to record CO<sub>2</sub> ( $\mu\text{mol CO}_2 \text{ mol}^{-1} \text{ air}$ ) and H<sub>2</sub>O ( $\text{mmol H}_2\text{O mol}^{-1} \text{ air}$ ) concentrations in the system logger ( $1 \text{ s}^{-1}$ ). Gap filling of missing data due to technical problems (i.e., 27% of the data across the study period between November 2015 and October 2016) was based on the average diurnal cycle of each month.

The rates of soil CO<sub>2</sub> flux,  $R_s$  ( $\mu\text{mol CO}_2 \text{ m}^{-2} \text{ s}^{-1}$ ), were calculated from chamber data using a linear fit of change in the water-corrected CO<sub>2</sub> mole fraction using Eq. (4) as follows:

$$R_s = \frac{dC}{dt} \cdot \frac{vP}{sT_aR}, \quad (4)$$

where  $dC/dt$  is the rate of change in the water-corrected CO<sub>2</sub> mol fraction ( $\mu\text{mol CO}_2 \text{ mol}^{-1} \text{ air s}^{-1}$ ),  $v$  is the system volume ( $\text{m}^3$ ),  $P$  is the chamber pressure (Pa),  $s$  is the soil surface area within the collar ( $\text{m}^2$ ),  $T_a$  is the chamber air temperature (K), and  $R$  is the gas constant ( $\text{J mol}^{-1} \text{ K}^{-1}$ ). A measurement period of 2 min was used, based on prelim-

inary tests to obtain the most linear increase of CO<sub>2</sub> in the chambers with the highest  $R^2$ .

Soil CO<sub>2</sub> fluxes in the experimental plot were measured between November 2015 and October 2016 by means of three measurement chambers using 21 collars grouped in seven sites in the forest stand, with three locations (i.e., three collars) per site, based on different distances from the nearest tree ( $D_t$ ). The collars were inserted 5 cm into the soil. Data were recorded on a half-hourly basis (48 daily records). The three chambers were rotated between the seven sites every 1–2 weeks to cover all sites and to assess spatial and temporal variations.

Upscaling of the collar measurements to plot-scale soil CO<sub>2</sub> flux was carried out by grouping collars based on three locations (i.e., under trees (< 1 m from nearest tree; UT), in gaps between trees (1–2.3 m; BT), and in open areas (> 2.3 m; OA)), with one chamber taking measurements at each location, and estimating the fractional areas ( $\varnothing$ ) of the three locations based on mapping the sites according to the distances noted above, as previously done by Raz-Yaseef et al. (2010):

$$R_s = R_{sOA} \cdot \varnothing_{OA} + R_{sBT} \cdot \varnothing_{BT} + R_{sUT} \cdot \varnothing_{UT}, \quad (5)$$

$$\varnothing_{OA} + \varnothing_{BT} + \varnothing_{UT} = 1. \quad (6)$$

The annual scale of  $R_s$  was derived from the upscaled chamber measurements (Eq. 5) based on daily records (48 half-hourly values) of spatially upscaled  $R_s$ .

Estimating the temperature sensitivity of  $R_s$  ( $Q_{10}$ ) was performed as described by Davidson and Janssens (2006) using a first-order exponential equation (see also Xu et al., 2015):

$$R_s = a e^{b T_s}, \quad (7)$$

where  $R_s$  represents the half-hourly spatially upscaled time series of soil respiration flux ( $\mu\text{mol m}^{-2} \text{s}^{-1}$ ),  $T_s$  ( $^{\circ}\text{C}$ ) is soil temperature at a 5 cm depth (upscaled spatially and temporally using the same method as for  $R_s$ ), and  $a$  and  $b$  are fitted parameters. The  $b$  values were used to calculate the  $Q_{10}$  value according to the following equation:

$$Q_{10} = e^{10b}. \quad (8)$$

## 2.4 Soil CO<sub>2</sub> flux partitioning

The determination of different sources of soil CO<sub>2</sub> efflux was based on linear mixing models (Lin et al., 1999) to estimate proportions of three main sources (autotrophic, heterotrophic, and abiotic), using isotopic analysis of soil CO<sub>2</sub> profiles and soil incubation data from eight campaigns (January to September) during 2016, according to Eqs. (9)–(11). Partitioning of the monthly  $R_s$  values into components was done using a three-end-member triangular model for interpreting the  $\delta^{13}\text{C}$  and  $\Delta^{14}\text{C}$  values of CO<sub>2</sub> flux; the three-end-member triangular corners are the autotrophic ( $R_{sa}$ ), heterotrophic ( $R_h$ ), and abiotic ( $R_i$ ) sources of  $R_s$ . The  $\delta^{13}\text{C}$  and

$\Delta^{14}\text{C}$  isotope signatures of monthly  $R_s$  locate it inside the triangle (Fig. S2):

$$\delta^{13}\text{C}_{R_s} = f_{sa} \cdot \delta^{13}\text{C}_{sa} + f_h \cdot \delta^{13}\text{C}_h + f_i \cdot \delta^{13}\text{C}_i, \quad (9)$$

$$\Delta^{14}\text{C}_{R_s} = f_{sa} \cdot \Delta^{14}\text{C}_{sa} + f_h \cdot \Delta^{14}\text{C}_h + f_i \cdot \Delta^{14}\text{C}_i, \quad (10)$$

$$1 = f_{sa} + f_h + f_i, \quad (11)$$

where  $f$  indicates the fraction of total soil flux (e.g.,  $f_h = R_h/R_s$ ), while subscripts sa, h, and i indicate autotrophic, heterotrophic, and inorganic components, respectively. The three-equations system was used to solve the three unknown  $f$  fractions of the total soil flux based on empirical estimates of the isotopic end-members. Additionally,  $\delta^{13}\text{C}$  and  $\Delta^{14}\text{C}$  are the stable and radioactive carbon isotopic ratios, where  $\delta^{13}\text{C} = [([^{13}\text{C}/^{12}\text{C}]_{\text{sample}}/[^{13}\text{C}/^{12}\text{C}]_{\text{reference}}) - 1] \cdot 1000\text{‰}$ , and the reference is the Vienna international standard (VPDB). Radiocarbon data are expressed as  $\Delta^{14}\text{C}$  in parts per thousand or per mil (‰), which is the deviation of a sample  $^{14}\text{C}/^{12}\text{C}$  ratio relative to the OxI standard in 1950 (see Taylor et al., 2015), that is,  $\Delta^{14}\text{C} = [([^{14}\text{C}/^{12}\text{C}]_{\text{sample}}/(0.95 \cdot [^{14}\text{C}/^{12}\text{C}]_{\text{reference}} \cdot \exp[(y - 1950)/8267])) - 1] \cdot 1000\text{‰}$ , where  $y$  is the year of sample measurements.

The  $\delta^{13}\text{C}_{R_s}$  was estimated monthly using the Keeling plot approach (Figs. S3 and S4; Pataki et al., 2003; Taneva and Gonzalez-Meler, 2011). Soil air was sampled using closed-end stainless-steel tubes (6 mm diameter) perforated near the tube bottom at four depths (30, 60, 90, and 120 cm). Samples of soil air were collected in pre-evacuated 150 mL glass flasks with high-vacuum valves, the dead volume in the tubing and flask necks having been purged with soil air using a plastic syringe equipped with a three-way valve.

Note that the Keeling plot approach is based on the two-end-member mixing model (see Review of Pataki et al., 2003), which often does not hold in soils because of variations in the  $\delta^{13}\text{C}$  values of source material with depth (see a recent example in Joseph et al., 2019). However, probably because of the very dry conditions at our study site, no change in  $\delta^{13}\text{C}$  with depths in the root zone is observed ( $\pm 0.1\text{‰}$  across the 35 cm depth profiles; Fig. S5), providing an opportunity to avoid this caveat; we must also conclude of course that the variations among the contributions of  $R_{sa}$ ,  $R_h$ , and  $R_i$  do not change significantly with depth, permitting the use of the single set of isotopic signatures in Table 2. The soil CO<sub>2</sub> samplings carried out therefore represented predominantly the mixing of atmospheric CO<sub>2</sub> with a single integrated soil source signal, consistent with the Keeling plot approach.

The autotrophic ( $\delta^{13}\text{C}_{sa}$ ) end-member was estimated based on incubations during the sampling periods of excised roots, following Carbone et al. (2008). Fine roots (< 2 mm diameter) were collected, rinsed with deionized water, and incubated for 3 h in 10 mL glass flasks connected with Swagelok Ultra-Torr tee fittings to 330 mL glass flasks

equipped with Louwers high-vacuum valves. The flasks were flushed with CO<sub>2</sub>-free air at room temperature close to field conditions. The CO<sub>2</sub> was allowed to accumulate to at least 2000 ppm (~ 2 h).

The heterotrophic ( $\delta^{13}\text{C}_h$ ) end-member was estimated as in Taylor et al. (2015), and, similar to the root-incubation experiment, soil samples from the top 5 cm of the litter layer or 10 cm below the soil surface were collected, and roots were carefully removed to isolate heterotrophic components. Root-free soils were placed in 10 mL glass flasks and allowed to incubate for 24 h before being transferred to evacuated 330 mL glass flasks. The inorganic source ( $\delta^{13}\text{C}_i$ ) end-member was estimated using 1 g of dry soil (ground to pass through a 0.5 mm mesh) placed in a 10 mL tube with a septum cap; then, 12 mL of 1 M HCl was added to dissolve the carbonate fraction, and the fumigated CO<sub>2</sub> withdrawn from each tube was collected using a 10 mL syringe and injected into a 330 mL evacuated flask for isotopic analysis.

Radiocarbon estimates were based on the work of Carmi et al. (2013) at the same site, adjusted to the measured atmospheric <sup>14</sup>C values during the study period (49.5‰; Carmi et al., 2013). The  $\Delta^{14}\text{C}_{\text{sa}}$  and  $\Delta^{14}\text{C}_h$  end-members were estimated based on the assumption that they carry the <sup>14</sup>C signatures of 4 and 8.5 years, respectively, older than the <sup>14</sup>C signature of the atmosphere at the time of sampling, based on mean ages previously estimated (Graven et al., 2012; Levin et al., 2010; Taylor et al., 2015). The ratio  $\Delta^{14}\text{C}_i$  was obtained from Carmi et al. (2013). Monthly values of  $\Delta^{14}\text{C}_{R_s}$  were obtained using the linear equation of the regression line of the measured  $\delta^{13}\text{C}$  values of  $R_{\text{sa}}$ ,  $R_{\text{sh}}$ , and  $R_i$  and the corresponding estimated  $\Delta^{14}\text{C}$  values (Fig. S2) and monthly  $\delta^{13}\text{C}$  values of  $R_s$ .

## 2.5 Isotopic analysis

Isotopic analysis followed the methodology described in Hemming et al. (2005). The  $\delta^{13}\text{C}$  of CO<sub>2</sub> in the air was analyzed using a continuous-flow mass spectrometer connected to a 15-flask automatic manifold system. An aliquot of 1.5 mL of air was expanded from each flask into a sampling loop on a 15-position valve (Valco, Houston, TX, USA). CO<sub>2</sub> was cryogenically trapped from the air samples using helium as a carrier gas; it was then separated from N<sub>2</sub>O with a Carbosieve G (Sigma-Aldrich) packed column at 70 °C and analyzed on a Europa 20-20 isotope ratio mass spectrometer (IRMS; Sercon, Crewe, UK). The  $\delta^{13}\text{C}$  results were quoted in parts per thousand (‰) relative to the VPDB international standard. The analytical precision was 0.1‰. To measure [CO<sub>2</sub>], an additional 40.0 mL subsample of air from each flask was expanded into mechanical bellows and then passed through an infrared gas analyzer (LI-6262; LI-COR, Lincoln, NE, USA) in an automated system. The precision of these measurements was 0.1 ppm. Flasks filled with calibrated standard air were measured with each batch of 10 sample flasks; five standards were measured per 10 samples for

$\delta^{13}\text{C}$  analyses and four standards per 10 samples for [CO<sub>2</sub>] analyses.

Organic matter samples were dried at 60 °C and milled using a Wiley mill fitted with a size 40 mesh, and soil samples were ground in a pestle and mortar. Soils containing carbonates were treated with 1 M hydrochloric acid. Between 0.2 and 0.4 mg of each dry sample was weighed into tin capsules (Elemental Microanalysis Ltd., Okehampton, UK), and the  $\delta^{13}\text{C}$  of each was determined using an elemental analyzer linked to a Micromass Optima IRMS (Manchester, UK). Three replicates of each sample were analyzed, and two samples of a laboratory working standard cellulose were measured for every 12 samples. Four samples of the acetanilide (Elemental Microanalysis Ltd.) international standard were used to calibrate each run, and a correction was applied to account for the influence of a blank cup. The precision was 0.1‰.

## 2.6 Total belowground carbon allocation (TBCA)

TBCA ( $\text{g C m}^{-2} \text{ yr}^{-1}$ ) was calculated following Giardina and Ryan (2002) for the study year (November 2015–October 2016) as follows:

$$\text{TBCA} = R_s - R_{\text{alp}} + \Delta\text{C}_{\text{soil}}, \quad (12)$$

where  $R_{\text{alp}}$  is the annual aboveground litter production between November 2014 and October 2015, and  $\Delta\text{C}_{\text{soil}}$  is the annual change in belowground total soil organic C. Litter production, not measured during the present study, was estimated based on values obtained by Masyk et al. (2008) for 2000–2006 ( $56 \text{ g C m}^{-2} \text{ yr}^{-1}$ ) and assumed to have increased in the study period (2014–2015) proportionally to the measured increase in leaf area index (LAI; 1.31 to 1.94; i.e.,  $R_{\text{alp}} = [(1.94 \cdot 56)/1.31] = 83 \text{ g C m}^{-2} \text{ yr}^{-1}$ ). For herbaceous litter production, three plots of 25 m<sup>2</sup> were randomly selected in 2002 and harvested at the end of the growing season, total fresh biomass was weighed, and subsamples were used to determine dry weight and C content. Grünzweig et al. (2007) found that herbaceous litter production was close to the average rainfall for the specific year; this method was adapted in the current study for the period between November 2014 and October 2015. Since aboveground litter ( $R_{\text{alp}}$ ; the sum of tree litter and herbaceous litter production) of a given year was mainly produced during that year but decayed during the following hydrological year, TBCA was based on the current year's  $R_s$  (2015–2016) and the previous year's  $R_{\text{alp}}$  (2014–2015).  $\Delta\text{C}_{\text{soil}}$  was set constant as the average annual belowground carbon increase since afforestation (Qubaja et al., 2019).

## 2.7 Statistical analyses

Two-way ANOVA tests were performed at a significance level set at  $p = 0.001$  to detect significant effects of locations (OA, BT, and UT), sites, and their interactions on  $R_s$

and meteorological parameters. Pearson correlation analysis ( $r$ ) was used to detect the correlation between  $R_s$  and meteorological parameters. To quantify spatiotemporal variability in  $R_s$ , the coefficient of variation (CV %) was calculated as  $[(\text{STDEV} / \text{Mean}) \cdot 100 \text{ \%}]$ . Heterogeneity was considered weak if  $\text{CV \%} \leq 10 \text{ \%}$ , moderate if  $10 \text{ \%} < \text{CV \%} \leq 100 \text{ \%}$ , and strong if  $\text{CV \%} > 100 \text{ \%}$ . All the analyses were performed using MATLAB software, Version R2017b (MathWorks, Inc., MA, USA).

### 3 Results

#### 3.1 Spatial variations

The spatial variations in  $R_s$  across locations (distance from nearest tree) and sites (across the study area) are reported in Table 1, together with other measured variables. The results indicated an overall mean  $R_s$  value of  $0.8 \pm 0.1 \mu\text{mol m}^{-2} \text{ s}^{-1}$ , with distinct values for the three locations.  $R_s$  was greater at UT locations than at the BT and OA locations by a factor of  $\sim 2$ . The spatial variability among the locations was also apparent in the  $R_s$  daily cycle (Fig. 1), with clear differences between the wet season (November to April), when the UT showed consistently higher  $R_s$  values than at other locations by a factor of about 1.6, and the dry season, when the equivalent values differed by a factor of approximately 2.6. Note that the daily peak in  $R_s$  remained at midday in both the wet and dry seasons. Overall, the 21 collars showed moderate variations ( $\text{CV} = 55 \text{ \%}$ ; Table 1);  $R_s$  was negatively correlated with distance from trees ( $D_i$ ;  $r = -0.62$ ;  $p < 0.01$ ) and with soil and air temperatures ( $T_s$  and  $T_a$ ;  $r = -0.45$ ;  $p < 0.05$ ) and positively correlated with soil water content and relative humidity (SWC and RH;  $r = 0.50$ ;  $p < 0.05$ ). The inverse correlation between  $R_s$  and distance from the nearest tree could be useful in considering the expected decline in stand density due to thinning and mortality (e.g., associated with a drying climate). For a first approximation, the results indicate that decreasing from the present stand density of 300 to 100 trees  $\text{ha}^{-1}$  and the resulting increase in mean distance among trees could result in decreasing ecosystem  $R_s$  by 11 %.

#### 3.2 Temporal dynamics

On the diurnal timescale, CO<sub>2</sub> fluxes showed typical daily cycles (Fig. 1). As expected, on average, all CO<sub>2</sub> fluxes were higher during the wet period compared to the dry season by a factor of  $\sim 2$ . However,  $R_s$  and  $R_e$  peaked around midday in both the wet and dry seasons, while the more physiologically controlled NEE and GPP showed a shift from midday (around 11:00–14:00 LT) to early morning (08:00–11:00 LT) in the dry season, with a midday depression and a secondary afternoon peak (Fig. 1d).

The temporal variations across the seasonal cycle are reported in Fig. 2, based on monthly mean values and exhibit-

ing sharp differences between the wet and dry seasons. As previously observed in this semiarid site, all CO<sub>2</sub> fluxes peak in early spring between March and April. The corresponding high-resolution data are reported in Fig. S6, which show also that the high winter (February)  $R_s$  rates were associated with clear days when photosynthetic active radiation (PAR) increased with air temperature,  $T_a$ . These data also show that, following rainy days, daily  $R_s$  values could reach  $6.1 \mu\text{mol m}^{-2} \text{ s}^{-1}$  (i.e., in the UT microsite; data not shown), although the average was  $1.1 \pm 0.2 \mu\text{mol m}^{-2} \text{ s}^{-1}$  during the wet period, which diminished by  $\sim 55 \text{ \%}$  in the dry season to mean daily values of  $0.5 \pm 0.1 \mu\text{mol m}^{-2} \text{ s}^{-1}$ . In spring (April), all CO<sub>2</sub> fluxes peaked during the crossover trends of decreasing soil moisture content and increasing temperature and PAR (Fig. S6).

The temporal variations in the half-hourly values of  $R_s$  reflected changes in soil moisture at 0–5 cm depth and PAR ( $r = 0.5$  and  $0.2$ , respectively;  $p < 0.01$ ) and negative correlations with  $T_s$  and RH ( $r = 0.2$  and  $0.1$ , respectively;  $p < 0.01$ ). The variations in the integrated  $R_s$  showed a CV of 71 %, with the temporal variations dominated strongly by PAR ( $\text{CV} > 100 \text{ \%}$ ), moderately by SWC ( $\text{CV} \sim 85 \text{ \%}$ ), and weakly by RH ( $\text{CV} \sim 40 \text{ \%}$ ; correlations and CV values were not included in figures and tables). Repeating the models applied by Grünzweig et al. (2009), the potential climatic factors that best predicted daily  $R_s$  shifted from SWC and PAR in the dry season to  $T_s$  and PAR in the wet season (Table S2). These equations explained 43 % and 70 % of the variation in  $R_s$  in the dry and wet seasons, respectively (Table S2). A reasonable forecast of the temporal variations in  $R_s$  ( $\mu\text{mol m}^{-2} \text{ s}^{-1}$ ) at half-hourly values ( $R^2 = 0.60$ ,  $p < 0.0001$ ) was obtained based on  $\text{SWC}_{0-10}$  and  $T_s$  values across the entire seasonal cycle, based on

$$R_s = 0.05126 \cdot \exp \left( 0.04274 \cdot T_s + 28.51 \cdot \text{SWC} - 74.44 \cdot \text{SWC}^2 \right). \quad (13)$$

At the ecosystem scale,  $R_e$  was characterized by high fluxes in the wet season and peak values of  $\sim 2.4 \mu\text{mol m}^{-2} \text{ s}^{-1}$  in February to April (Fig. 2; Table S1).  $R_e$  fluxes rapidly decreased after the cessation of rain and reached the lowest values in the fall (September to October), with mean dry-period values of  $0.5 \pm 0.1 \mu\text{mol m}^{-2} \text{ s}^{-1}$  (Fig. 2, Table S1). GPP had a mean value of  $-1.8 \pm 0.4 \mu\text{mol m}^{-2} \text{ s}^{-1}$ , and daily NEE had a mean value of  $-0.5 \pm 0.3 \mu\text{mol m}^{-2} \text{ s}^{-1}$  (Table S1 and Fig. S6), with the same seasonality for both (Fig. 2).

Figure 3 (see also Table 2) summarizes the seasonal variations in  $R_s$  and  $R_e$  partitioning. The monthly  $R_{sa}$  and  $R_h$  were not significantly different but were significantly different from  $R_i$  ( $p < 0.05$ ). The  $R_{sa}/R_s$  ratios ranged from 0.32 to 0.46, the largest contribution occurring in early spring from February to April. The  $R_h/R_s$  fraction ranged between 0.33 and 0.45, being the highest during the wet season. The  $R_i/R_s$

**Table 1.** Annual mean of half-hourly values across locations (OA, open area; BT, between trees; UT, under tree) in seven sites in the forest during the study period of soil respiration flux rates ( $R_s$ ) together with the soil water content at 10 cm depth (SWC), minimum distances from nearby tree ( $D_t$ ), soil temperature at 5 cm depth ( $T_s$ ), and air temperature ( $T_a$ ) and relative humidity (RH) at the soil surface (numbers in parentheses indicate  $\pm$ SE).

Locations	Sites	$R_s$ ( $\mu\text{mol m}^{-2} \text{s}^{-1}$ )	SWC ( $\times 100 \text{ m}^3 \text{ m}^{-3}$ )	$D_t$ (m)	$T_s$ ( $^{\circ}\text{C}$ )	$T_a$ ( $^{\circ}\text{C}$ )	RH (%)
OA	1	1.64 (0.02)	16.5 (0.2)	2.9	15.6 (0.1)	15.4 (0.2)	59.7 (0.5)
	2	0.72 (0.01)	14.5 (0.2)	3.6	15.9 (0.2)	15.0 (0.2)	58.4 (0.6)
	3	1.23 (0.02)	19.3 (0.2)	7.0	20.6 (0.3)	18.2 (0.2)	53.5 (0.5)
	4	0.38 (0.01)	11.3 (0.2)	3.0	22.6 (0.2)	20.8 (0.1)	58.9 (0.4)
	5	0.38 (0.01)	5.8 (0.2)	3.0	25.5 (0.1)	24.0 (0.1)	43.1 (0.4)
	6	0.31 (0.01)	5.7 (0.4)	2.8	30.0 (0.3)	26.2 (0.3)	51.8 (0.9)
	7	0.14 (0.01)	6.1 (0.3)	3.5	25.5 (0.2)	23.2 (0.3)	44.5 (0.9)
	Average CV (%)	0.68 (0.21) 81 %	11 (0) 50 %	3.7 (0.6) 41 %	22.3 (2.0)	20.4 (1.6)	52.8 (2.6) 13 %
BT	1	0.77 (0.01)	10.5 (0.2)	1.8	16.1 (0.1)	15.2 (0.2)	60.5 (0.5)
	2	0.88 (0.01)	12.1 (0.2)	1.5	14.8 (0.2)	14.7 (0.2)	59.5 (0.6)
	3	0.84 (0.01)	20.4 (0.2)	2.7	20.1 (0.3)	18.4 (0.2)	54.1 (0.6)
	4	0.91 (0.01)	14.4 (0.2)	2.7	23.3 (0.2)	21.3 (0.2)	58.5 (0.4)
	5	0.41 (0.00)	3.9 (0.2)	2.0	24.6 (0.1)	24.0 (0.1)	43.2 (0.4)
	6	0.41 (0.01)	3.3 (0.4)	2.5	29.1 (0.2)	26.0 (0.3)	52.5 (0.8)
	7	0.46 (0.01)	5.5 (0.3)	1.2	23.9 (0.1)	22.8 (0.3)	45.7 (0.9)
	Average CV (%)	0.67 (0.09) 35 %	10 (0) 63 %	2.0 (0.2) 29 %	21.7 (1.9)	20.3 (1.6)	53.4 (2.6) 13 %
UT	1	1.22 (0.02)	9.3 (0.2)	0.2	15.7 (0.1)	15.2 (0.2)	60.0 (0.5)
	2	1.42 (0.01)	14.0 (0.2)	0.3	14.8 (0.2)	14.8 (0.2)	59.4 (0.6)
	3	1.64 (0.01)	19.8 (0.2)	0.5	19.0 (0.2)	18.0 (0.2)	54.5 (0.6)
	4	1.90 (0.02)	11.3 (0.2)	0.6	22.0 (0.1)	20.8 (0.1)	59.0 (0.4)
	5	1.16 (0.01)	4.0 (0.2)	0.4	23.9 (0.1)	23.7 (0.1)	44.1 (0.4)
	6	1.29 (0.01)	4.5 (0.4)	0.2	29.5 (0.3)	25.9 (0.3)	52.7 (0.9)
	7	0.89 (0.01)	5.2 (0.3)	0.2	25.0 (0.1)	23.0 (0.3)	45.5 (0.9)
	Average CV (%)	1.36 (0.13) 25 %	10 (0) 60 %	0.3 (0.1) 46 %	21.4 (2.0)	20.2 (1.6)	53.6 (2.5) 12 %
All	Average (SE)	0.8 (0.1)	11 (0)	2.0 (0.4)	21.8 (1.1)	20.3 (0.9)	53.3 (1.4)
	Max	1.90	20	7.0	30.0	26.2	60.5
	Min	0.14	3	0.2	14.8	14.7	43.1
	CV (%)	55 %	55 %	82 %			12 %
Two-way ANOVA ( <i>P</i> value)	Site	0.000	0.000		0.000	0.000	0.000
	Location	0.000	0.000		0.000	0.220	0.074
	Site $\times$ location	0.000	0.000		0.000	0.645	0.961
Pearson Correlation with $R_s$			0.50*	-0.62**	-0.45*	-0.45*	0.50*

\* Correlation is significant at the 0.05 level (two-tailed). \*\* Correlation is significant at the 0.01 level (two-tailed).

fraction – the fraction of inorganic sources from the total soil respiration – ranged from 0.09 to 0.35, the largest contribution being in the driest period. The mean relative contributions of these components to  $R_s$  over the sampling campaigns are presented in Fig. 3a, but, on average, soil biotic fluxes were higher than abiotic fluxes by a factor of  $\sim 4$ .  $R_e$  partitioning showed an average increase in  $R_f/R_e$  from 25 % in the wet season to 54 % in the dry season and a decline in

$R_s/R_e$  from 75 % to 46 % on average from the wet to the dry season, respectively, which reflected a seasonal change of  $R_f$  in the wet season to peak values in the dry season (Fig. 3b). Both the highest and lowest  $R_s$  fractions ( $\sim 0.74$  and nearly 0.34) along the seasonal cycle were associated with low total  $R_e$  fluxes, that is, in the fall before the  $R_f$  peak in the spring and in the summer, when physiological controls limited water loss (Fig. 2).

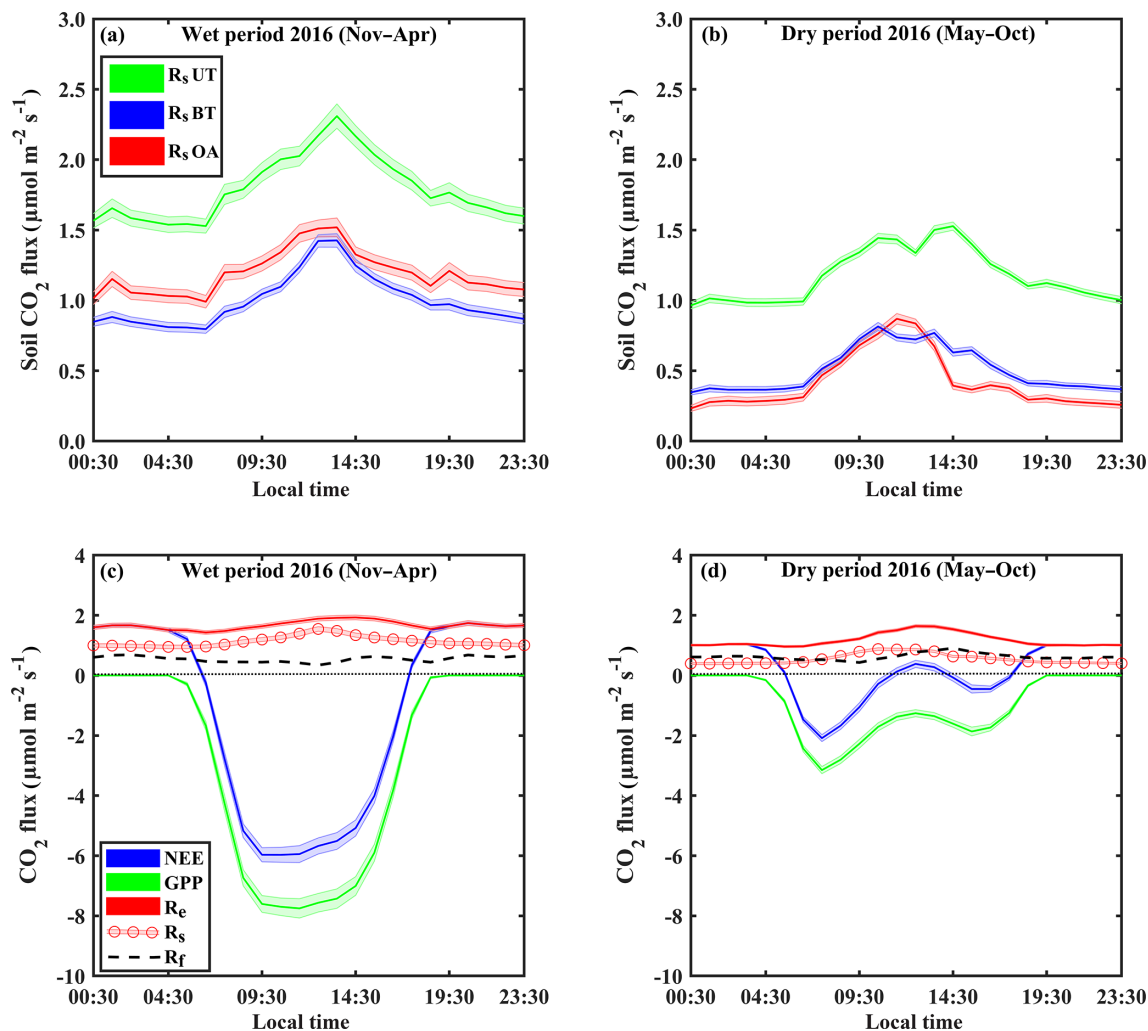


**Figure 1.** Representative diurnal cycles of soil respiration ( $R_s$ ; using soil chambers across locations: open area, OA; between trees, BT; under trees, UT) and sites in panels (a) and (b), of net ecosystem exchange (NEE; canopy-scale eddy covariance) and gross primary production (GPP) and ecosystem respiration ( $R_e$ ) and its partitioning to soil respiration ( $R_s$ ) and aboveground tree respiration ( $R_f$ ) in panels (c) and (d), during the wet (November–April) and dry (May–October) periods. Based on half-hourly values over the diurnal cycle; shaded areas indicate  $\pm$ SE;  $R_f$  was estimated as the residual as  $R_f = R_e - R_s$  and is presented as a dashed line.

**Table 2.** The  $\delta^{13}\text{C}$  and  $\Delta^{14}\text{C}$  signature of soil respiration ( $R_s$ ) and its partitioning into autotrophic ( $R_{sa}$ ), heterotrophic ( $R_h$ ), and abiotic ( $R_i$ ), together with the relative contribution of each to the soil and ecosystem respiration for Yatir Forest during eight campaigns of measurements from January to September 2016 (numbers in parentheses indicate  $\pm$ SE) in comparison to results obtained previously in the same forest (2001–2006 mean values). The monthly contribution of  $R_{sa}$ ,  $R_h$ , and  $R_i$  to  $R_s$  or  $R_e$  is presented in Fig. 3a and b, respectively.

Signature	$R_{sa}$	$R_h$	$R_i$	$R_s$
	(%o)			
$\delta^{13}\text{C}$	$-23.7 (0.5)^1$	$-24.3 (0.0)^1$	$-6.5 (0.0)^1$	$-20.8 (\pm 0.6)^1$
$\Delta^{14}\text{C}$	$30^3$	$50^3$	$-900^2$	$-134 (34)^4$
Relative contribution to $R_s$ (2015–2016)	0.40 (0.02)	0.39 (0.02)	0.21 (0.04)	
Relative contribution to $R_e$ (2015–2016)	0.24 (0.04)	0.23 (0.04)	0.13 (0.01)	0.60 (0.06)

<sup>1</sup> Measured in the present study. <sup>2</sup> Measured by Carmi et al. (2013). <sup>3</sup> Calculated based on the measured atmospheric value by Carmi et al. (2013). <sup>4</sup> Calculated based on the best-fit regression equation in Fig. S2.

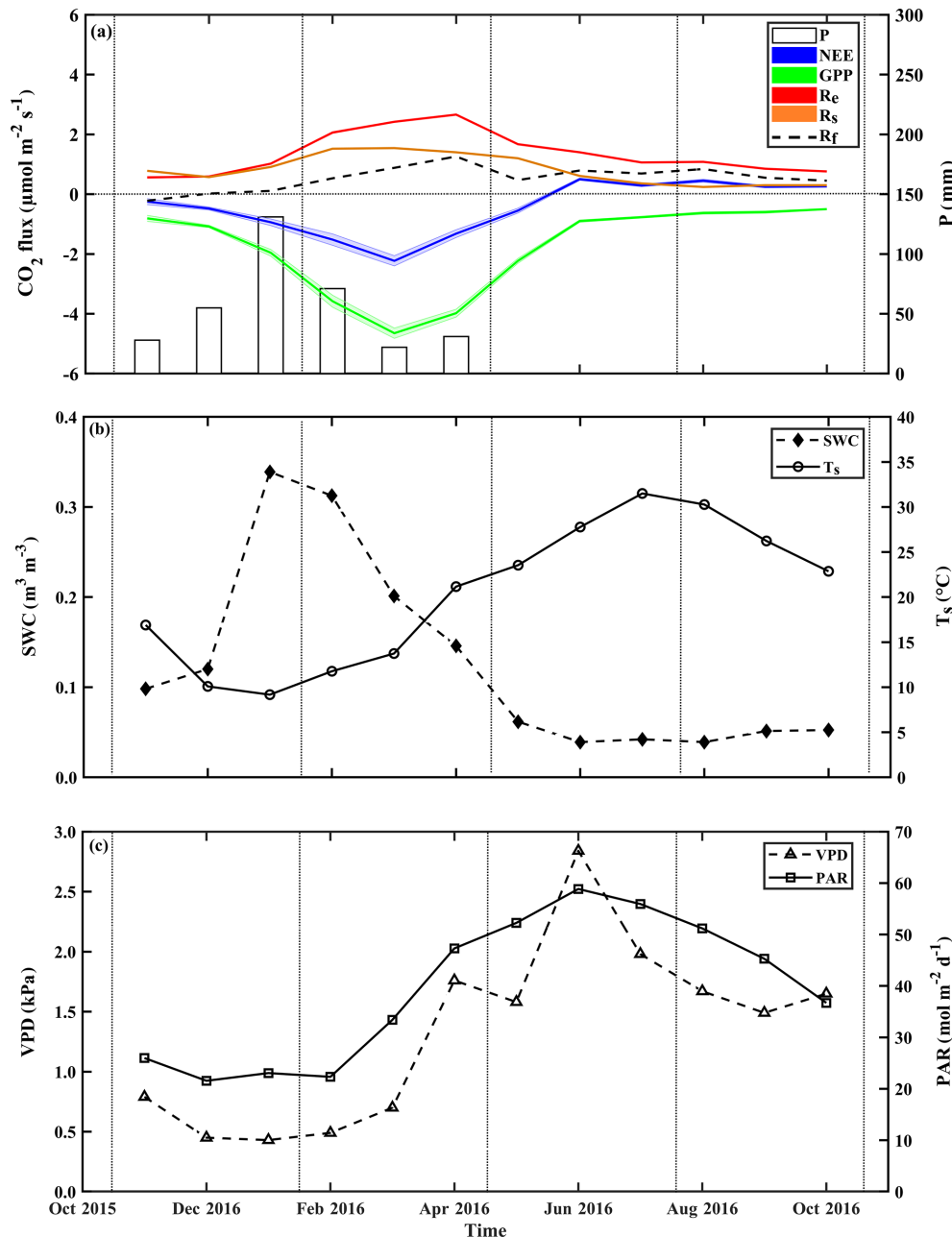


**Figure 2.** Seasonal trends of monthly mean values during the research period of (a) the fluxes of net ecosystem exchange (NEE), gross primary production (GPP), and ecosystem respiration ( $R_e$ ) and its components, soil respiration ( $R_s$ ) and aboveground tree respiration ( $R_f$ ), and monthly mean of precipitation (P), and monthly mean of key environmental parameters; (b) soil water content at the top 10 cm ( $SWC_{0-10}$ ) and soil temperature at 5 cm ( $T_s$ ); and (c) vapor pressure deficit (VPD) and photosynthetic activity radiation (PAR).  $R_f$  is obtained from  $R_e - R_s$ . Vertical dotted lines indicate the winter, spring, summer, and fall seasons.

### 3.3 Annual scale

On an annual timescale, estimates of CO<sub>2</sub> flux components based on EC measurements resulted in annual values of GPP, NPP,  $R_e$ , and NEP of 655, 282, 488, and 167 g C m<sup>-2</sup> yr<sup>-1</sup>, respectively (Tables 3 and S1). On average across the measurement period,  $R_s$  was the main CO<sub>2</sub> flux to atmosphere,

making up  $60 \pm 6\%$  of  $R_e$  ( $295 \pm 4$  g C m<sup>-2</sup> yr<sup>-1</sup>; Tables 3 and S1), and  $R_f$  was another significant component accounting for  $40 \pm 6\%$  of  $R_e$  (Fig. 3b), which reflected the low-density ( $300$  trees ha<sup>-1</sup>) nature of the semiarid forest. As indicated above,  $R_e$  partitioning showed a decrease in  $R_s/R_e$  and an increase in  $R_f/R_e$  from winter to summer, which is clearly apparent in Fig. 3b. On an annual scale, during the

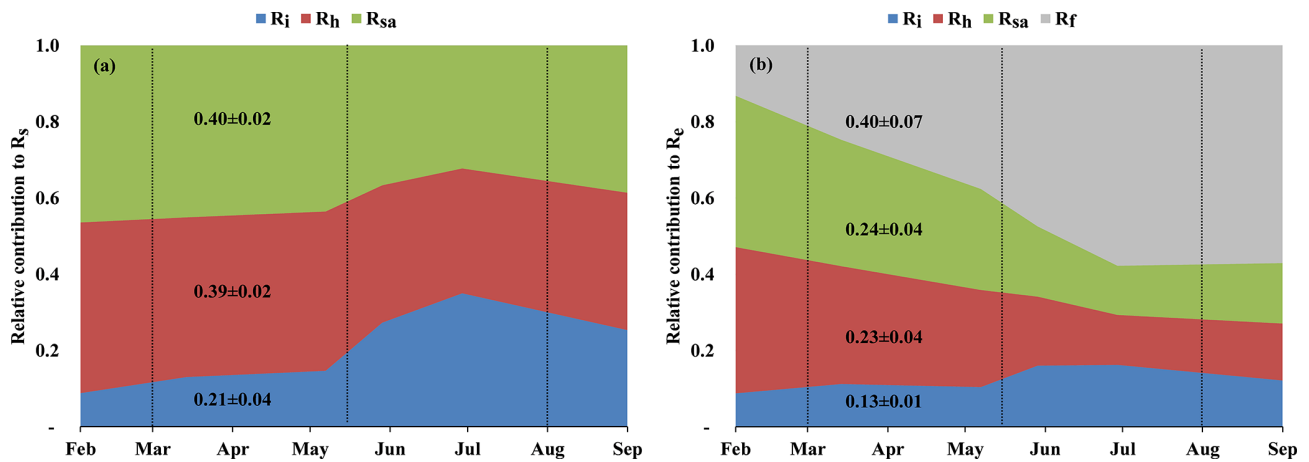


**Figure 3.** (a) Seasonal variations in the relative contribution of soil autotrophic ( $R_{sa}$ ), heterotrophic ( $R_h$ ), and abiotic ( $R_i$ ) components to  $R_s$ , and (b) seasonal variations in the relative contribution of soil autotrophic ( $R_{sa}$ ), heterotrophic ( $R_h$ ), abiotic ( $R_i$ ), and foliage and stem respiration ( $R_f$  is obtained from  $R_e - R_s$ ) components to ecosystem respiration ( $R_e$ ) during eight campaigns (January–September) in 2016. The contributions were estimated with linear mixing models using  $\delta^{13}\text{C}$  and  $\Delta^{14}\text{C}$  of soil respiration ( $R_s$ ) and a soil CO<sub>2</sub> profile method at 0 to 120 cm soil depth. Vertical dotted lines indicate the winter, spring, summer, and fall seasons. These results confirmed earlier estimates of Grünzweig et al. (2009) and Maseyk et al. (2008a).

**Table 3.** Mean annual values of ecosystem respiration ( $R_e$ ), its components and associated ratios, net ecosystem exchange (NEE; from eddy covariance), net primary productivity (NPP), gross primary productivity (GPP), carbon-use efficiency (CUE), leaf area index (LAI), and ratio of total belowground carbon allocation (TBCA) to GPP (TBCA / GPP) in the present study (mean of November 2015 to October 2016) and in comparison to results obtained previously in the same forest (2001–2006 mean values).  $R_i$ ,  $R_h$ ,  $R_{sa}$ ,  $R_s$ ,  $R_l$  and  $R_w$  denote abiotic, heterotrophic, soil autotrophic, soil, foliage, and wood CO<sub>2</sub> flux, respectively.  $Q_{10}$  is derived during the two studies for the wet and dry seasons.

Study	$R_s$	$R_h$	$R_{sa}$	$R_l$	$R_w$	$R_i$	$R_e$	NEE	NPP	GPP
	(g m <sup>-2</sup> yr <sup>-1</sup> )									
Mean (2001–2006)	406	147	203	260	70	56	735	−211	−358	−880
$x/R_s$		0.36	0.50			0.14				
$x/R_e$	0.55	0.20	0.28	0.35	0.10	0.07				
Mean (2015–2016)	295	115	119	155	39	61	488	−167	−282	−655
$x/R_s$		0.39	0.40			0.21				
$x/R_e$	0.60	0.23	0.24	0.32	0.08	0.13				
Ratio of $(x/R_s)_{2016}/(x/R_s)_{2003}$		1.08	0.81			1.50				
Ratio of $(x/R_e)_{2016}/(x/R_e)_{2003}$	1.09	1.18	0.88	0.90	0.84	1.64				
Study	$Q_{10}$		CUE	TBCA / GPP <sup>3</sup>	LAI					
	SWC <sup>1</sup>	SWC <sup>2</sup>								
Mean (2001–2006)	2.5	1.2	0.40	0.41	1.3					
Mean (2015–2016)	1.6	1.1	0.43	0.38	2.1					
Ratio of $x_{2016}/x_{2003}$	0.64	0.92	1.06	0.93	1.62					

<sup>1</sup> SWC  $\geq 0.2$  (m<sup>3</sup> m<sup>-3</sup>). <sup>2</sup> SWC < 0.2 (m<sup>3</sup> m<sup>-3</sup>). <sup>3</sup> The mean of GPP used by Grünzweig et al. (2009) to estimate the TBCA / GPP ratio was 834 g m<sup>-2</sup> yr<sup>-1</sup>.

study period, estimates of  $R_f$ ,  $R_{sa}$ ,  $R_h$ , and  $R_i$  values were  $194 \pm 36$ ,  $119 \pm 21$ ,  $115 \pm 20$ , and  $61 \pm 6 \text{ g C m}^{-2} \text{ yr}^{-1}$ , respectively. These rates of respiration fluxes translated at the ecosystem scale to  $R_e / \text{GPP}$  of  $\sim 75 \%$ , lower than observed in other ecosystems (Table S3) and leading, in turn, to high ecosystem CUE of 0.43.

Using the site records of nearly 20 years, long-term trends in GPP, NPP,  $R_e$ , and NEP were examined. Soil respiration and its partitioning could not be similarly monitored continuously, but combining the present results with the 2001–2006 values obtained by Grünzweig et al. (2009) and Maseyk et al. (2008a) provided a basis for estimating the long-term trends in soil respiration. Notably, no clear or significant trend over time was observed in any of the canopy-scale continuously monitored fluxes, but, because of relatively large interannual variations, associated mainly with those in precipitation (see Qubaja et al., 2020), it is likely that the relative contributions of the different fluxes, expressed as ratios in Table 3, provide a more robust perspective of the long-term temporal changes in the ecosystem functioning. The results presented in Table 3 reflect the long-term growth of the forest, with a relatively large increase in LAI, but the TBCA remained around 40%. The results also indicated little change in the total soil respiration,  $R_s$ , component, (as a fraction of  $R_e$  or GPP) but a general shift from the autotrophic components to the heterotrophic component (i.e.,  $R_h$ ). This was reflected in the decreasing ratio of the autotrophic components (i.e.,  $R_{sa}$ ,  $R_l$ , and  $R_w$ ) and the increasing ratio of  $R_h$  to  $R_e$  (Table 3) across the 13-year observation period (2003 to 2016).

#### 4 Discussion

Partitioning ecosystem carbon fluxes and long-term observational studies are key to understanding ecosystem carbon dynamics and their response to change. Overall, the results support our research hypothesis that the observed high CUE at our site is at least partly due to the characteristics of the carbon flux partitioning that can be associated with the semiarid conditions. Compared to other sites and climates (see comparative compilation in Table S3 in the Supplement), the results reflect several key points: (1) relatively high belowground allocation; (2) low soil respiration in general and low heterotrophic respiration in particular; (3) combining the results for 2016 and those of our earlier study offered a long-term perspective across 13 years, indicating that the low  $R_s$  in this ecosystem is robust and exhibits reduced sensitivity to temperature; and (4) there is a general long-term shift from autotrophic to heterotrophic respiration.

Comparing CO<sub>2</sub> fluxes in this forest with fluxes in a range of European forests showed that mean NEP in the semiarid forest ( $167 \text{ g C m}^{-2} \text{ yr}^{-1}$ ) is similar to the mean NEP in other European forests ( $150 \text{ g C m}^{-2} \text{ yr}^{-1}$ ; FLUXNET).

Carbon partitioning belowground (TBCA/GPP) was relatively high ( $\sim 38 \%$ ), with little change across the long-term observation period. It is, however, within the range of mean values for forests in different biomes (Litton et al., 2007). High belowground allocation helps explain the high rate of SOC (soil organic carbon) accumulation observed over the period since afforestation (Grünzweig et al., 2007; Qubaja et al., 2019). Note that, irrespective of the soil carbon accumulation, the abiotic component to the CO<sub>2</sub> flux seems to be significant in dry environments (Table 3) and in particular in the dry seasons, when biological activities drastically decrease (Kowalski et al., 2008; Lopez-Ballesteros et al., 2017; Serrano-Ortiz et al., 2010; Martí-Roura et al., 2019). The results show that considering the abiotic effects on estimating soil respiration and, in turn, on estimating the carbon budget in dry calcareous soils can play an important part in estimating soil and ecosystem respiration fluxes (Angert et al., 2015; Roland et al., 2012).

The soil CO<sub>2</sub> efflux in the semiarid forest ( $295 \text{ g C m}^{-2} \text{ yr}^{-1}$ ) is at the low end of  $R_s$  values across the range of climatic regions, from 50 to  $2750 \text{ g C m}^{-2} \text{ yr}^{-1}$  (Adachi et al., 2017; Chen et al., 2014; Grünzweig et al., 2009; Hashimoto et al., 2015). This is clearly lower than the mean  $R_s$  value for global evergreen needle forests, which is estimated at  $690 \text{ g C m}^{-2} \text{ yr}^{-1}$  (Chen et al., 2014), and between estimates for desert scrub and Mediterranean woodland ( $224\text{--}713 \text{ g C m}^{-2} \text{ yr}^{-1}$ ; Raich and Schlesinger, 1992) or for Mediterranean forests ( $561\text{--}1,015 \text{ g C m}^{-2} \text{ yr}^{-1}$ ; Casals et al., 2011; Luyssaert et al., 2007; Matteucci et al., 2015; Misson et al., 2010; Rey et al., 2002; Rodeghiero and Cescatti, 2005). The mean instantaneous rate of  $R_s$ ,  $0.8 \mu\text{mol m}^{-2} \text{ s}^{-1}$ , is also in the range reported for unmanaged forest and grassland in the dry Mediterranean region ( $0.5$  and  $2.1 \mu\text{mol m}^{-2} \text{ s}^{-1}$ ; Correia et al., 2012).

The observed low  $R_s$  values were associated with a relatively high fraction of autotrophic and a lower fraction of heterotrophic respiration. The mean annual-scale  $R_{sa}/R_s$  ratio of 0.40 was at the high end of the global range of 0.09 to 0.49 (Chen et al., 2014; Hashimoto et al., 2015). In contrast, heterotrophic respiration showed an annual-scale  $R_h/R_s$  ratio of  $0.39 \pm 0.02$  (Table 2 and Fig. 3), which is lower than the estimated global mean  $R_h/R_s$  value of 0.56 (Hashimoto et al., 2015) but within the range of Mediterranean region forest, which varies between 0.29 and 0.77 (Casals et al., 2011; Luyssaert et al., 2007; Matteucci et al., 2015; Misson et al., 2010; Rey et al., 2002; Rodeghiero and Cescatti, 2005). The relatively low annual scale of the heterotrophic respiration to  $R_s$  is consistent with the dry soil over much of the year in this forest (Figs. 2 and S6) and the observed low decomposability of plant detritus and the high mean SOC accumulation rate (Grünzweig et al., 2007).

The long-term perspective from the 13-year observation period indicates emerging trends that can be a basis for assessing the effects of forest age and the evident increase in LAI (Table 3) and changes in environmental conditions (gen-

erally warming and drying; see, e.g., Lelieveld et al., 2012). Here, because comparing the noncontinuous data from the present (2016) and earlier (2001–2006) studies is sensitive to the large interannual variations in the ecosystem activities and fluxes (Qubaja et al., 2019), we focused on the more robust changes in the ratio of the respiration components to the overall fluxes ( $R_e$ ; Table 3). This shows a shifting trend from the autotrophic components to the heterotrophic, with little change in the contribution of  $R_s$  to the overall efflux. The ratios of  $R_{sa}$ ,  $R_l$ , and  $R_w$  to  $R_e$  tended to decrease by about 13 %, while that of  $R_h$  increased by about 18 %; similar trends were seen in soil respiration, with  $R_{sa}/R_s$  decreasing by  $-19$  % and  $R_h/R_s$  increasing by  $+8$  % (Table 3). The relatively low  $R_s$  under conditions of high temperature in the semiarid ecosystem implies reduced sensitivity of respiration to temperature. This is partly imposed by low SWC conditions during extended parts of the year (Grünzweig et al., 2009; cf. Rey et al., 2002; Xu and Qi, 2001). Accordingly,  $R_s$  showed greater sensitivity to  $T_s$  in the wet period, but, during the 8–9 months of the year when SWC was below  $\sim 0.2 \text{ m}^3 \text{ m}^{-3}$ ,  $R_s$  varied predominantly with water availability. The long-term perspective reported in Table 3 indicates a further decrease in temperature sensitivity, with mean  $Q_{10}$  values in the dry season decreasing from 1.6 to 1.1. These estimated  $Q_{10}$  values are generally consistent with published values for different ecosystems (1.4 to 2.0; Hashimoto et al., 2015; Zhou et al., 2009) and with low values under low SWC (Reichstein et al., 2003; Tang et al., 2005). This is also consistent with soil warming experiments by  $0.76$  °C in Mediterranean ecosystems, which decreased the  $R_s$  by 16 % and  $Q_{10}$  by 14 % (Wang et al., 2014). Note also that the low temperature sensitivity in the dry season is likely to be related to reduced microbial activity but may also involve downregulation of plant activity (Maseyk et al., 2008a) and drought-induced dormancy of shallow roots (Schiller, 2000). Finally, we also note that the greater importance of moisture availability in influencing respiration is clearly apparent from the observed relationships of  $R_s$  and  $R_h$  to mean annual precipitation (MAP) in European evergreen needle forests (Fig. S8; see also Grünzweig et al., 2007), which are not observed with respect to mean annual temperature.

**Data availability.** The data used in this study are archived and available from the corresponding author upon request (dan.yakir@weizmann.ac.il).

**Supplement.** The supplement related to this article is available online at: <https://doi.org/10.5194/bg-17-699-2020-supplement>.

**Author contributions.** RQ and DY designed the study; RQ, FT, ER, and DY performed the experiments. RQ and DY analyzed the data.

RQ and DY wrote the paper, with discussions and contributions to interpretations of the results from all the coauthors.

**Competing interests.** The authors declare that they have no conflict of interest.

**Acknowledgements.** This long-term study was funded by the Forestry Department of Keren Kayemeth LeIsrael (KKL) and the German Research Foundation (DFG) as part of the project “Climate feedbacks and benefits of semi-arid forests” (CliFF), by the Israel Science Foundation (ISF; grant no. 1976/17), and by the Israel Science Foundation and the National Natural Science Foundation of China (ISF–NSFC) joint research program (grant no. 2579/16). The authors thank Efrat Schwartz for assistance with lab work. The long-term operation of the Yatir Forest Research Field Site is supported by the Cathy Wills and Robert Lewis Program in Environmental Science. We thank the entire Yatir team for technical support and the local KKL personnel for their cooperation.

**Financial support.** This research has been supported by the Forestry Department of Keren Kayemeth LeIsrael (KKL) and the German Research Foundation (DFG) as part of the project “Climate feedbacks and benefits of semi-arid forests” (CliFF), the Israel Science Foundation (ISF; grant no. 1976/17), and the National Natural Science Foundation of China (ISF–NSFC) joint research program (grant no. 2579/16).

**Review statement.** This paper was edited by Frank Hagedorn and reviewed by two anonymous referees.

## References

- Adachi, M., Ito, A., Yonemura, S., and Takeuchi, W.: Estimation of global soil respiration by accounting for land-use changes derived from remote sensing data, *J. Environ. Manage.*, 200, 97–104, <https://doi.org/10.1016/j.jenvman.2017.05.076>, 2017.
- Angert, A., Yakir, D., Rodeghiero, M., Preisler, Y., Davidson, E. A., and Weiner, T.: Using O<sub>2</sub> to study the relationships between soil CO<sub>2</sub> efflux and soil respiration, *Biogeosciences*, 12, 2089–2099, <https://doi.org/10.5194/bg-12-2089-2015>, 2015.
- Aubinet, M., Grelle, A., Ibrom, A., Rannik, U., Moncrieff, J., Foken, T., Kowalski, A. S., Martin, P. H., Berbigier, P., Bernhofer, C., Clement, R., Elbers, J., Granier, A., Grunwald, T., Morgenstern, K., Pilegaard, K., Rebmann, C., Snijders, W., Valentini, R., and Vesala, T.: Estimates of the annual net carbon and water exchange of forests: The EUROFLUX methodology, *Adv. Ecol. Res.*, 30, 113–175, 2000.
- Bahn, M., Janssens, I. A., Reichstein, M., Smith, P., and Trumbore, S. E.: Soil respiration across scales: towards an integration of patterns and processes, *New Phytol.*, 186, 292–296, <https://doi.org/10.1111/j.1469-8137.2010.03237.x>, 2010.
- Balogh, J., Pinter, K., Foti, S., Cserhalmi, D., Papp, M., and Nagy, Z.: Dependence of soil respiration on soil mois-

- ture, clay content, soil organic matter, and CO<sub>2</sub> uptake in dry grasslands, *Soil Biol. Biochem.*, 43, 1006–1013, <https://doi.org/10.1016/j.soilbio.2011.01.017>, 2011.
- Binkley, D., Stape, J. L., Takahashi, E. N., and Ryan, M. G.: Tree-girdling to separate root and heterotrophic respiration in two Eucalyptus stands in Brazil, *Oecologia*, 148, 447–454, <https://doi.org/10.1007/s00442-006-0383-6>, 2006.
- Bonan, G. B.: *Ecological climatology: concepts and applications*, 2nd Edn., Cambridge: Cambridge University Press, Cambridge, 28–37, 2008.
- Bond-Lamberty, B. and Thomson, A.: Temperature-associated increases in the global soil respiration record, *Nature*, 464, 579–582, <https://doi.org/10.1038/nature08930>, 2010.
- Buchmann, N.: Biotic and abiotic factors controlling soil respiration rates in *Picea abies* stands, *Soil Biol. Biochem.*, 32, 1625–1635, [https://doi.org/10.1016/s0038-0717\(00\)00077-8](https://doi.org/10.1016/s0038-0717(00)00077-8), 2000.
- Carbone, M. S., Winston, G. C., and Trumbore, S. E.: Soil respiration in perennial grass and shrub ecosystems: Linking environmental controls with plant and microbial sources on seasonal and diel timescales, *J. Geophys. Res.-Biogeo.*, 113, G02022, <https://doi.org/10.1029/2007jg000611>, 2008.
- Carmi, I., Yakir, D., Yechieli, Y., Kronfeld, J., and Stiller, M.: Variations in soil CO<sub>2</sub> concentrations and isotopic values in a semi-arid region due to biotic and abiotic processes in the unsaturated zone, *Radiocarbon*, 55, 932–942, 2013.
- Carvalho, N., Forkel, M., Khomik, M., Bellarby, J., Jung, M., Migliavacca, M., Mu, M. Q., Saatchi, S., Santoro, M., Thurner, M., Weber, U., Ahrens, B., Beer, C., Cescatti, A., Randerson, J. T., and Reichstein, M.: Global covariation of carbon turnover times with climate in terrestrial ecosystems, *Nature*, 514, 213–217, <https://doi.org/10.1038/nature13731>, 2014.
- Casals, P., Lopez-Sangil, L., Carrara, A., Gimeno, C., and Nogues, S.: Autotrophic and heterotrophic contributions to short-term soil CO<sub>2</sub> efflux following simulated summer precipitation pulses in a Mediterranean dehesa, *Global Biogeochem. Cy.*, 25, GB3012, <https://doi.org/10.1029/2010gb003973>, 2011.
- Chen, D., Zhang, Y., Lin, Y., Zhu, W., and Fu, S.: Changes in belowground carbon in *Acacia crassicarpa* and *Eucalyptus urophylla* plantations after tree girdling, *Plant Soil*, 326, 123–135, <https://doi.org/10.1007/s11104-009-9986-0>, 2010.
- Chen, S. T., Zou, J. W., Hu, Z. H., Chen, H. S., and Lu, Y. Y.: Global annual soil respiration in relation to climate, soil properties and vegetation characteristics: Summary of available data, *Agr. Forest Meteorol.*, 198, 335–346, <https://doi.org/10.1016/j.agrformet.2014.08.020>, 2014.
- Conant, R. T., Klopatek, J. M., Malin, R. C., and Klopatek, C. C.: Carbon pools and fluxes along an environmental gradient in northern Arizona, *Biogeochemistry*, 43, 43–61, <https://doi.org/10.1023/a:1006004110637>, 1998.
- Correia, A. C., Minunno, F., Caldeira, M. C., Banza, J., Mateus, J., Carneiro, M., Wingate, L., Shvaleva, A., Ramos, A., Jongen, M., Bugalho, M. N., Nogueira, C., Lecomte, X., and Pereira, J. S.: Soil water availability strongly modulates soil CO<sub>2</sub> efflux in different Mediterranean ecosystems: Model calibration using the Bayesian approach, *Agr. Ecosyst. Environ.*, 161, 88–100, <https://doi.org/10.1016/j.agee.2012.07.025>, 2012.
- Davidson, E. A. and Janssens, I. A.: Temperature sensitivity of soil carbon decomposition and feedbacks to climate change, *Nature*, 440, 165–173, <https://doi.org/10.1038/nature04514>, 2006.
- DeLucia, E. H., Drake, J. E., Thomas, R. B., and Gonzalez-Meler, M.: Forest carbon use efficiency: is respiration a constant fraction of gross primary production?, *Glob. Change Biol.*, 13, 1157–1167, <https://doi.org/10.1111/j.1365-2486.2007.01365.x>, 2007.
- Deng, Q., Hui, D., Zhang, D., Zhou, G., Liu, J., Liu, S., Chu, G., and Li, J.: Effects of Precipitation Increase on Soil Respiration: A Three-Year Field Experiment in Subtropical Forests in China, *Plos One*, 7, e41493, <https://doi.org/10.1371/journal.pone.0041493>, 2012.
- Etzold, S., Ruehr, N. K., Zweifel, R., Dobbertin, M., Zingg, A., Pluess, P., Hasler, R., Eugster, W., and Buchmann, N.: The Carbon Balance of Two Contrasting Mountain Forest Ecosystems in Switzerland: Similar Annual Trends, but Seasonal Differences, *Ecosystems*, 14, 1289–1309, <https://doi.org/10.1007/s10021-011-9481-3>, 2011.
- Etzold, S., Zweifel, R., Ruehr, N. K., Eugster, W., and Buchmann, N.: Long-term stem CO<sub>2</sub> concentration measurements in Norway spruce in relation to biotic and abiotic factors, *New Phytol.*, 197, 1173–1184, <https://doi.org/10.1111/nph.12115>, 2013.
- Falge, E., Baldocchi, D., Tenhunen, J., Aubinet, M., Bakwin, P., Berbigier, P., Bernhofer, C., Burba, G., Clement, R., Davis, K. J., Elbers, J. A., Goldstein, A. H., Grelle, A., Granier, A., Guomundsson, J., Hollinger, D., Kowalski, A. S., Katul, G., Law, B. E., Malhi, Y., Meyers, T., Monson, R. K., Munger, J. W., Oechel, W., Paw, K. T., Pilegaard, K., Rannik, U., Rebmann, C., Suyker, A., Valentini, R., Wilson, K., and Wofsy, S.: Seasonality of ecosystem respiration and gross primary production as derived from FLUXNET measurements, *Agr. Forest Meteorol.*, 113, 53–74, [https://doi.org/10.1016/s0168-1923\(02\)00102-8](https://doi.org/10.1016/s0168-1923(02)00102-8), 2002.
- Flechard, C. R., Ibrom, A., Skiba, U. M., de Vries, W., van Oijen, M., Cameron, D. R., Dise, N. B., Korhonen, J. F. J., Buchmann, N., Legout, A., Simpson, D., Sanz, M. J., Aubinet, M., Loustau, D., Montagnani, L., Neiryck, J., Janssens, I. A., Pihlatie, M., Kiese, R., Siemens, J., Francez, A.-J., Augustin, J., Varlagin, A., Olejnik, J., Juszczak, R., Aurela, M., Chojnicki, B. H., Dämmgen, U., Djuricic, V., Drewer, J., Eugster, W., Fauvel, Y., Fowler, D., Frumau, A., Granier, A., Gross, P., Hamon, Y., Helfter, C., Hensen, A., Horváth, L., Kitzler, B., Kruijt, B., Kutsch, W. L., Lobo-do-Vale, R., Lohila, A., Longdoz, B., Marek, M. V., Matteucci, G., Mitisinkova, M., Moreaux, V., Nefel, A., Ourcival, J.-M., Pilegaard, K., Pita, G., Sanz, F., Schjoerring, J. K., Sebastià, M.-T., Tang, Y. S., Uggerud, H., Urbaniak, M., van Dijk, N., Vesala, T., Vidic, S., Vincke, C., Weidinger, T., Zechmeister-Boltenstern, S., Butterbach-Bahl, K., Nemitz, E., and Sutton, M. A.: Carbon / nitrogen interactions in European forests and semi-natural vegetation. Part I: Fluxes and budgets of carbon, nitrogen and greenhouse gases from ecosystem monitoring and modelling, *Biogeosciences Discuss.*, <https://doi.org/10.5194/bg-2019-333>, in review, 2019a.
- Flechard, C. R., van Oijen, M., Cameron, D. R., de Vries, W., Ibrom, A., Buchmann, N., Dise, N. B., Janssens, I. A., Neiryck, J., Montagnani, L., Varlagin, A., Loustau, D., Legout, A., Ziemlińska, K., Aubinet, M., Aurela, M., Chojnicki, B. H., Drewer, J., Eugster, W., Francez, A.-J., Juszczak, R., Kitzler, B., Kutsch, W. L., Lohila, A., Longdoz, B., Matteucci, G., Moreaux, V., Nefel, A., Olejnik, J., Sanz, M. J., Siemens, J., Vesala, T., Vincke, C., Nemitz, E., Zechmeister-Boltenstern, S., Butterbach-Bahl, K., Skiba, U. M., and Sutton, M. A.: Carbon / nitrogen interactions in European forests and semi-natural vegetation. Part II:

- Untangling climatic, edaphic, management and nitrogen deposition effects on carbon sequestration potentials, *Biogeosciences Discuss.*, <https://doi.org/10.5194/bg-2019-335>, in review, 2019b.
- Frank, A. B., Liebig, M. A., and Hanson, J. D.: Soil carbon dioxide fluxes in northern semiarid grasslands, *Soil Biol. Biochem.*, 34, 1235–1241, [https://doi.org/10.1016/s0038-0717\(02\)00062-7](https://doi.org/10.1016/s0038-0717(02)00062-7), 2002.
- Frey, B., Hagedorn, F., and Giudici, F.: Effect of girdling on soil respiration and root composition in a sweet chestnut forest, *Forest Ecol. Manage.*, 225, 271–277, <https://doi.org/10.1016/j.foreco.2006.01.003>, 2006.
- Gelfand, I., Grünzweig, J. M., and Yakir, D.: Slowing of nitrogen cycling and increasing nitrogen use efficiency following afforestation of semi-arid shrubland, *Oecologia*, 168, 563–575, <https://doi.org/10.1007/s00442-011-2111-0>, 2012.
- Giardina, C. P. and Ryan, M. G.: Total belowground carbon allocation in a fast-growing Eucalyptus plantation estimated using a carbon balance approach, *Ecosystems*, 5, 487–499, <https://doi.org/10.1007/s10021-002-0130-8>, 2002.
- Graven, H. D., Guilderson, T. P., and Keeling, R. F.: Observations of radiocarbon in CO<sub>2</sub> at La Jolla, California, USA 1992–2007: Analysis of the long-term trend, *J. Geophys. Res.-Atmos.*, 117, D02302, <https://doi.org/10.1029/2011jd016533>, 2012.
- Grünzweig, J. M., Gelfand, I., Fried, Y., and Yakir, D.: Biogeochemical factors contributing to enhanced carbon storage following afforestation of a semi-arid shrubland, *Biogeosciences*, 4, 891–904, <https://doi.org/10.5194/bg-4-891-2007>, 2007.
- Grünzweig, J. M., Hemming, D., Maseyk, K., Lin, T., Rotenberg, E., Raz-Yaseef, N., Falloon, P. D., and Yakir, D.: Water limitation to soil CO<sub>2</sub> efflux in a pine forest at the semi-arid “timberline”, *J. Geophys. Res.-Biogeo.*, 114, G03008, <https://doi.org/10.1029/2008jg000874>, 2009.
- Grünzweig, J. M., Lin, T., Rotenberg, E., Schwartz, A., and Yakir, D.: Carbon sequestration in arid-land forest, *Glob. Change Biol.*, 9, 791–799, <https://doi.org/10.1046/j.1365-2486.2003.00612.x>, 2003.
- Hagedorn, F., Joseph, J., Peter, M., Luster, J., Pritsch, K., Gepfert, U., Kerner, R., Molinier, V., Egli, S., Schaub, M., Liu, J. F., Li, M. H., Sever, K., Weiler, M., Siegwolf, R. T. W., Gessler, A., and Arend, M.: Recovery of trees from drought depends on belowground sink control, *Nat. Plants*, 2, 1–5, <https://doi.org/10.1038/nplants.2016.111>, 2016.
- Hashimoto, S., Carvalhais, N., Ito, A., Migliavacca, M., Nishina, K., and Reichstein, M.: Global spatiotemporal distribution of soil respiration modeled using a global database, *Biogeosciences*, 12, 4121–4132, <https://doi.org/10.5194/bg-12-4121-2015>, 2015.
- Hemming, D., Yakir, D., Ambus, P., Aurela, M., Besson, C., Black, K., Buchmann, N., Burlett, R., Cescatti, A., Clement, R., Gross, P., Granier, A., Grunwald, T., Havrankova, K., Janous, D., Janssens, I. A., Knohl, A., Ostner, B. K., Kowalski, A., Laurila, T., Mata, C., Marcolla, B., Matteucci, G., Moncrieff, J., Moors, E. J., Osborne, B., Pereira, J. S., Pihlatie, M., Pilegaard, K., Ponti, F., Rosova, Z., Rossi, F., Scartazza, A., and Vesala, T.: Pan-European delta C-13 values of air and organic matter from forest ecosystems, *Glob. Change Biol.*, 11, 1065–1093, <https://doi.org/10.1111/j.1365-2486.2005.00971.x>, 2005.
- Hogberg, P., Bhupinderpal, S., Lofvenius, M. O., and Nordgren, A.: Partitioning of soil respiration into its autotrophic and heterotrophic components by means of tree-girdling in old boreal spruce forest, *Forest Ecol. Manage.*, 257, 1764–1767, <https://doi.org/10.1016/j.foreco.2009.01.036>, 2009.
- Hui, D. F. and Luo, Y. Q.: Evaluation of soil CO<sub>2</sub> production and transport in Duke Forest using a process-based modeling approach, *Global Biogeochem. Cy.*, 18, GB4029, <https://doi.org/10.1029/2004gb002297>, 2004.
- IPCC: Climate Change 2014: Mitigation of Climate Change, Contribution of Working Group III to the Fifth Assessment Report of the Intergovernmental Panel on Climate Change, edited by: Edenhofer, O., PichsMadruga, R., Sokona, Y., Minx, J. C., Farahani, E., Kadner, S., Seyboth, K., Adler, A., Baum, I., Brunner, S., Eickemeier, P., Kriemann, B., Savolainen, J., Schlomer, S., VonStechow, C., and Zwickel, T., Cambridge University Press, Cambridge and New York, 843–846, 2014.
- Jiang, H., Deng, Q., Zhou, G., Hui, D., Zhang, D., Liu, S., Chu, G., and Li, J.: Responses of soil respiration and its temperature/moisture sensitivity to precipitation in three subtropical forests in southern China, *Biogeosciences*, 10, 3963–3982, <https://doi.org/10.5194/bg-10-3963-2013>, 2013.
- Joseph, J., Kulls, C., Arend, M., Schaub, M., Hagedorn, F., Gessler, A., and Weiler, M.: Application of a laser-based spectrometer for continuous in situ measurements of stable isotopes of soil CO<sub>2</sub> in calcareous and acidic soils, *Soil*, 5, 49–62, <https://doi.org/10.5194/soil-5-49-2019>, 2019.
- Kowalski, A. S., Serrano-Ortiz, P., Janssens, I. A., Sanchez-Moral, S., Cuezva, S., Domingo, F., Were, A., and Alados-Arboledas, L.: Can flux tower research neglect geochemical CO<sub>2</sub> exchange?, *Agr. Forest Meteorol.*, 148, 1045–1054, <https://doi.org/10.1016/j.agrformet.2008.02.004>, 2008.
- Kuzyakov, Y.: Sources of CO<sub>2</sub> efflux from soil and review of partitioning methods, *Soil Biol. Biochem.*, 38, 425–448, <https://doi.org/10.1016/j.soilbio.2005.08.020>, 2006.
- Lelieveld, J., Hadjinicolaou, P., Kostopoulou, E., Chenoweth, J., El Maayar, M., Giannakopoulos, C., Hannides, C., Lange, M. A., Tanarhte, M., Tyrlis, E., and Xoplaki, E.: Climate change and impacts in the Eastern Mediterranean and the Middle East, *Climatic Change*, 114, 667–687, <https://doi.org/10.1007/s10584-012-0418-4>, 2012.
- Lellei-Kovacs, E., Kovacs-Lang, E., Botta-Dukat, Z., Kalapos, T., Emmett, B., and Beier, C.: Thresholds and interactive effects of soil moisture on the temperature response of soil respiration, *Eur. J. Soil Biol.*, 47, 247–255, <https://doi.org/10.1016/j.ejsobi.2011.05.004>, 2011.
- Levin, I., Naegler, T., Kromer, B., Diehl, M., Francey, R. J., Gomez-Pelaez, A. J., Steele, L. P., Wagenbach, D., Weller, R., and Worthy, D. E.: Observations and modelling of the global distribution and long-term trend of atmospheric (CO<sub>2</sub>)-C-14, *Tellus B*, 62, 207–207, <https://doi.org/10.1111/j.1600-0889.2010.00456.x>, 2010.
- Lin, G. H., Ehleringer, J. R., Rygielwicz, P. T., Johnson, M. G., and Tingey, D. T.: Elevated CO<sub>2</sub> and temperature impacts on different components of soil CO<sub>2</sub> efflux in Douglas-fir terracosms, *Glob. Change Biol.*, 5, 157–168, <https://doi.org/10.1046/j.1365-2486.1999.00211.x>, 1999.
- Litton, C. M., Raich, J. W., and Ryan, M. G.: Carbon allocation in forest ecosystems, *Glob. Change Biol.*, 13, 2089–2109, <https://doi.org/10.1111/j.1365-2486.2007.01420.x>, 2007.
- Lopez-Ballesteros, A., Serrano-Ortiz, P., Kowalski, A. S., Sanchez-Canete, E. P., Scott, R. L., and Domingo, F.: Subterranean

- ventilation of allochthonous CO<sub>2</sub> governs net CO<sub>2</sub> exchange in a semiarid Mediterranean grassland, *Agr. Forest Meteorol.*, 234, 115–126, <https://doi.org/10.1016/j.agrformet.2016.12.021>, 2017.
- Luyssaert, S., Inghima, I., Jung, M., Richardson, A. D., Reichstein, M., Papale, D., Piao, S. L., Schulzes, E. D., Wingate, L., Matteucci, G., Aragao, L., Aubinet, M., Beers, C., Bernhofer, C., Black, K. G., Bonal, D., Bonnefond, J. M., Chambers, J., Ciais, P., Cook, B., Davis, K. J., Dolman, A. J., Gielen, B., Goulden, M., Grace, J., Granier, A., Grelle, A., Griffis, T., Grunwald, T., Guidolotti, G., Hanson, P. J., Harding, R., Hollinger, D. Y., Hutyra, L. R., Kolar, P., Kruijt, B., Kutsch, W., Lagergren, F., Laurila, T., Law, B. E., Le Maire, G., Lindroth, A., Loustau, D., Malhi, Y., Mateus, J., Migliavacca, M., Misson, L., Montagnani, L., Moncrieff, J., Moors, E., Munger, J. W., Nikinmaa, E., Ollinger, S. V., Pita, G., Rebmann, C., Rouspard, O., Saigusa, N., Sanz, M. J., Seufert, G., Sierra, C., Smith, M. L., Tang, J., Valentini, R., Vesala, T., and Janssens, I. A.: CO<sub>2</sub> balance of boreal, temperate, and tropical forests derived from a global database, *Glob. Change Biol.*, 13, 2509–2537, <https://doi.org/10.1111/j.1365-2486.2007.01439.x>, 2007.
- Marti-Roura, M., Hagedorn, F., Rovira, P., and Romanya, J.: Effect of land use and carbonates on organic matter stabilization and microbial communities in Mediterranean soils, *Geoderma*, 351, 103–115, <https://doi.org/10.1016/j.geoderma.2019.05.021>, 2019.
- Maseyk, K., Grünzweig, J. M., Rotenberg, E., and Yakir, D.: Respiration acclimation contributes to high carbon-use efficiency in a seasonally dry pine forest, *Glob. Change Biol.*, 14, 1553–1567, <https://doi.org/10.1111/j.1365-2486.2008.01604.x>, 2008.
- Matteucci, M., Gruening, C., Ballarin, I. G., Seufert, G., and Cescatti, A.: Components, drivers and temporal dynamics of ecosystem respiration in a Mediterranean pine forest, *Soil Biol. Biochem.*, 88, 224–235, <https://doi.org/10.1016/j.soilbio.2015.05.017>, 2015.
- Misson, L., Rocheteau, A., Rambal, S., Ourcival, J. M., Limousin, J. M., and Rodriguez, R.: Functional changes in the control of carbon fluxes after 3 years of increased drought in a Mediterranean evergreen forest?, *Glob. Change Biol.*, 16, 2461–2475, <https://doi.org/10.1111/j.1365-2486.2009.02121.x>, 2010.
- Pataki, D. E., Ehleringer, J. R., Flanagan, L. B., Yakir, D., Bowling, D. R., Still, C. J., Buchmann, N., Kaplan, J. O., and Berry, J. A.: The application and interpretation of Keeling plots in terrestrial carbon cycle research, *Global Biogeochem. Cy.*, 17, 1022, <https://doi.org/10.1029/2001gb001850>, 2003.
- Peterjohn, W. T., Melillo, J. M., Steudler, P. A., Newkirk, K. M., Bowles, F. P., and Aber, J. D.: Responses of trace gas fluxes and N availability to experimentally elevated soil temperatures, *Ecol. Appl.*, 4, 617–625, <https://doi.org/10.2307/1941962>, 1994.
- Poulter, B., Frank, D., Ciais, P., Myneni, R. B., Andela, N., Bi, J., Broquet, G., Canadell, J. G., Chevallier, F., Liu, Y. Y., Running, S. W., Sitch, S., and van der Werf, G. R.: Contribution of semi-arid ecosystems to interannual variability of the global carbon cycle, *Nature*, 509, 600–603, <https://doi.org/10.1038/nature13376>, 2014.
- Preisler, Y., Tatarinov, F., Grünzweig, J. M., Bert, D., Ogee, J., Wingate, L., Rotenberg, E., Rohatyn, S., Her, N., Moshe, I., Klein, T., and Yakir, D.: Mortality versus survival in drought-affected Aleppo pine forest depends on the extent of rock cover and soil stoniness, *Funct. Ecol.*, 33, 901–912, <https://doi.org/10.1111/1365-2435.13302>, 2019.
- Qubaja, R., Grünzweig, J., Rotenberg, E., and Yakir, D.: Evidence for large carbon sink and long residence time in semiarid forests based on 15 year flux and inventory records, *Glob. Change Biol.*, 2019, 1–12, <https://doi.org/10.1111/gcb.14927>, 2019.
- Qubaja, R., Amer, M., Tatarinov, F., Rotenberg, E., Preisler, Y., Sprintsin, M., and Yakir, D.: Partitioning evapotranspiration and its long-term evolution in a dry pine forest using measurement-based estimates of soil evaporation, *Agr. Forest Meteorol.*, 281, 107831, <https://doi.org/10.1016/j.agrformet.2019.107831>, 2020.
- Raich, J. W. and Schlesinger, W. H.: The global carbon-dioxide flux in soil respiration and its relationship to vegetation and climate, *Tellus B*, 44, 81–99, <https://doi.org/10.1034/j.1600-0889.1992.t01-1-00001.x>, 1992.
- Ramnarine, R., Wagner-Riddle, C., Dunfield, K. E., and Voroney, R. P.: Contributions of carbonates to soil CO<sub>2</sub> emissions, *Can. J. Soil Sci.*, 92, 599–607, <https://doi.org/10.4141/cjss2011-025>, 2012.
- Raz-Yaseef, N., Rotenberg, E., and Yakir, D.: Effects of spatial variations in soil evaporation caused by tree shading on water flux partitioning in a semi-arid pine forest, *Agr. Forest Meteorol.*, 150, 454–462, <https://doi.org/10.1016/j.agrformet.2010.01.010>, 2010.
- Reichstein, M., Rey, A., Freibauer, A., Tenhunen, J., Valentini, R., Banza, J., Casals, P., Cheng, Y. F., Grünzweig, J. M., Irvine, J., Joffre, R., Law, B. E., Loustau, D., Miglietta, F., Oechel, W., Ourcival, J. M., Pereira, J. S., Peressotti, A., Ponti, F., Qi, Y., Rambal, S., Rayment, M., Romanya, J., Rossi, F., Tedeschi, V., Tirone, G., Xu, M., and Yakir, D.: Modeling temporal and large-scale spatial variability of soil respiration from soil water availability, temperature and vegetation productivity indices, *Global Biogeochem. Cy.*, 17, 1104, <https://doi.org/10.1029/2003gb002035>, 2003.
- Rey, A., Pegoraro, E., Tedeschi, V., De Parri, I., Jarvis, P. G., and Valentini, R.: Annual variation in soil respiration and its components in a coppice oak forest in Central Italy, *Glob. Change Biol.*, 8, 851–866, <https://doi.org/10.1046/j.1365-2486.2002.00521.x>, 2002.
- Rodeghiero, M. and Cescatti, A.: Main determinants of forest soil respiration along an elevation/temperature gradient in the Italian Alps, *Glob. Change Biol.*, 11, 1024–1041, <https://doi.org/10.1111/j.1365-2486.2005.00963.x>, 2005.
- Roland, M.: Contributions of carbonate weathering to the net ecosystem carbon balance of a mediterranean forest, Ph.D. thesis, Antwerpen University, Antwerpen, Belgium, 117–142, 2012.
- Ross, I., Misson, L., Rambal, S., Arneth, A., Scott, R. L., Carrara, A., Cescatti, A., and Genesio, L.: How do variations in the temporal distribution of rainfall events affect ecosystem fluxes in seasonally water-limited Northern Hemisphere shrublands and forests?, *Biogeosciences*, 9, 1007–1024, <https://doi.org/10.5194/bg-9-1007-2012>, 2012.
- Rotenberg, E. and Yakir, D.: Contribution of Semi-Arid Forests to the Climate System, *Science*, 327, 451–454, <https://doi.org/10.1126/science.1179998>, 2010.
- Schiller, G.: Ecophysiology of *Pinus halepensis* Mill. and *P. brutia* Ten, in: *Ecology, Biogeography and Management of Pinus halepensis and P. brutia Forest Ecosystems in the Mediterranean Basin*, edited by: Ne'eman, G. and Trabaud, L., Backhuys, Leiden, The Netherlands, 51–65, 2000.

- Serrano-Ortiz, P., Roland, M., Sanchez-Moral, S., Janssens, I. A., Domingo, F., Godderis, Y., and Kowalski, A. S.: Hidden, abiotic CO<sub>2</sub> flows and gaseous reservoirs in the terrestrial carbon cycle: Review and perspectives, *Agr. Forest Meteorol.*, 150, 321–329, <https://doi.org/10.1016/j.agrformet.2010.01.002>, 2010.
- Shachnovich, Y., Berliner, P. R., and Bar, P.: Rainfall interception and spatial distribution of throughfall in a pine forest planted in an arid zone, *J. Hydrol.*, 349, 168–177, <https://doi.org/10.1016/j.jhydrol.2007.10.051>, 2008.
- Shen, W. J., Jenerette, G. D., Hui, D. F., Phillips, R. P., and Ren, H.: Effects of changing precipitation regimes on dryland soil respiration and C pool dynamics at rainfall event, seasonal and interannual scales, *J. Geophys. Res.-Biogeo.*, 113, G03024, <https://doi.org/10.1029/2008jg000685>, 2008.
- Subke, J.-A., Voke, N. R., Leronni, V., Garnett, M. H., and Ineson, P.: Dynamics and pathways of autotrophic and heterotrophic soil CO<sub>2</sub> efflux revealed by forest girdling, *J. Ecol.*, 99, 186–193, <https://doi.org/10.1111/j.1365-2745.2010.01740.x>, 2011.
- Taneva, L. and Gonzalez-Meler, M. A.: Distinct patterns in the diurnal and seasonal variability in four components of soil respiration in a temperate forest under free-air CO<sub>2</sub> enrichment, *Biogeosciences*, 8, 3077–3092, <https://doi.org/10.5194/bg-8-3077-2011>, 2011.
- Tang, J. W., Baldocchi, D. D., and Xu, L.: Tree photosynthesis modulates soil respiration on a diurnal time scale, *Glob. Change Biol.*, 11, 1298–1304, <https://doi.org/10.1111/j.1365-2486.2005.00987.x>, 2005.
- Tatarinov, F., Rotenberg, E., Maseyk, K., Ogee, J., Klein, T., and Yakir, D.: Resilience to seasonal heat wave episodes in a Mediterranean pine forest, *New Phytol.*, 210, 485–496, <https://doi.org/10.1111/nph.13791>, 2016.
- Taylor, A. J., Lai, C. T., Hopkins, F. M., Wharton, S., Bible, K., Xu, X. M., Phillips, C., Bush, S., and Ehleringer, J. R.: Radiocarbon-Based Partitioning of Soil Respiration in an Old-Growth Coniferous Forest, *Ecosystems*, 18, 459–470, <https://doi.org/10.1007/s10021-014-9839-4>, 2015.
- Wang, X., Liu, L. L., Piao, S. L., Janssens, I. A., Tang, J. W., Liu, W. X., Chi, Y. G., Wang, J., and Xu, S.: Soil respiration under climate warming: differential response of heterotrophic and autotrophic respiration, *Glob. Change Biol.*, 20, 3229–3237, <https://doi.org/10.1111/gcb.12620>, 2014b.
- Xu, M. and Qi, Y.: Soil-surface CO<sub>2</sub> efflux and its spatial and temporal variations in a young ponderosa pine plantation in northern California, *Glob. Change Biol.*, 7, 667–677, <https://doi.org/10.1046/j.1354-1013.2001.00435.x>, 2001.
- Xu, Z. F., Tang, S. S., Xiong, L., Yang, W. Q., Yin, H. J., Tu, L. H., Wu, F. Z., Chen, L. H., and Tan, B.: Temperature sensitivity of soil respiration in China's forest ecosystems: Patterns and controls, *Appl. Soil Ecol.*, 93, 105–110, <https://doi.org/10.1016/j.apsoil.2015.04.008>, 2015.
- Zhou, T., Shi, P. J., Hui, D. F., and Luo, Y. Q.: Global pattern of temperature sensitivity of soil heterotrophic respiration ( $Q_{10}$ ) and its implications for carbon-climate feedback, *J. Geophys. Res.-Biogeo.*, 114, G02016, <https://doi.org/10.1029/2008jg000850>, 2009.